LA--12320-MS

DE93 006301

Material Science Experience Gained from the Space Nuclear Rocket Program: Insulators

Paul Wagner

Los Alamos
NATIONAL LABORATORY

Preface

In one of his last recorded educational television broadcasts, Nobel Laureate Richard Feynman observed that the generation of new knowledge is a slow, and often painful, process. This was certainly true in the Rover Program. Not only was our way beset with uncertainties in what materials to use and how to make them, but there were equally troublesome questions of how to evaluate the materials we had. The thermal conductivity of Rover materials is one illustration. The 1961 *Thermophysical Properties Research Center Handbook*, published by Purdue University, showed that the reported values for the thermal conductivity of graphite (the material we used most extensively in Rover) at room temperature varied by a factor of 10 000. It was clear that we did not know how to uniquely characterize the materials we were using, and moreover our measurement methods for thermal conductivity were not totally credible. The point to this is to emphasize that this report is a judgmental distillation of knowledge gained through approximately 75 manyears of research to define materials of engineering value, make those materials, and then verify their properties through thermophysical measurements. While detailed documentation of these activities would occupy several volumes, we feel that all the essential technological information can be transferred by this report.

The author received his Ph.D. in physical chemistry in 1952 from the University of Rochester. He performed research in materials science and high-temperature thermophysical measurements for the Rover Program from early 1956 until the program was abandoned in 1973. Largely as a result of these research efforts, he received the International Thermal Conductivity Award in 1989: only the sixteenth such award in the past 30 years. This recognition is a tribute to the vigorous effort exerted by the scientists and engineers involved in Rover as well as a recognition of the accomplishments of the individual.

MATERIAL SCIENCE EXPERIENCE GAINED FROM THE SPACE NUCLEAR ROCKET PROGRAM : INSULATORS

by

Paul Wagner

ABSTRACT

Although Rover reactors are viewed as the ultimate in high-temperature operating systems, many of the materials used in these reactors (for example, support rods, control drums, and the reflector) have to be held at relatively low temperatures while the reactor operates, in order to maintain their structural integrity. Thus the insulators needed to separate these temperature domains are crucial to the reactor's ultimate operating times and temperatures. All of the reactors that were tested used pyrolytic graphite as the primary insulator. However, it had been long planned to replace the graphite with zirconium carbide and a lengthy and intensive effort to develop the zirconium carbide insulators had been made at the time Rover was terminated. This report details research and development and the experience we gained with both these insulator materials.

I. INTRODUCTION

One of the primary goals of the 1955-1972 nuclear rocket propulsion (Rover) program was the development of reactors capable of heating hydrogen to an extremely high temperature to obtain a much higher engine specific impulse than the 400-500 s^{-1} obtainable from chemical rocket engines. The long-range goal for the temperature of the nuclear engine chamber was approximately 3000 K, but short-range goals were more modest, progressively increasing from about 2000 K to 2500 K. Near the end of the program, average fuel element exit-gas temperatures slightly above 2500 K were demonstrated during reactor tests. Coupled with the need for high temperature is the requirement for a sufficient engine lifetime to allow it to perform one or more missions. Thus, at least a portion of the reactor fuel and associated core components must be able to operate at temperatures at least slightly greater than the hydrogen chamber temperatures for 1 to 10 hours. On the other hand, the best materials for other reactor components can survive only at much lower temperatures. Therefore, there is a need for an insulating material in several reactor locations that can both withstand the high-temperature-hydrogen environment and sharply reduce the heat load to the low-temperature components. Furthermore, the thermal conductivity of the insulator should be as low as possible so that the insulator does not take up too much space. The progressive development of nuclear-rocket-reactor fuel elements able to operate at higher temperatures for longer times has been described in several recent publications. The purpose of this report is to describe the accompanying developments in insulators, which are also vital to improvements in nuclear engine performance.

These high-temperature insulator applications in Rover reactors are shown in Fig. 1. In Fig. 1a, the insulator reduces the heat flow to the metallic components of the core axial-support system; in Fig. 1b, the insulator protects the aft end of the support system; and in Fig. 1c, the insulator protects reactor components at the radial edge of the core.

The use of pyrographite (PyG or PyC for pyrolytic carbon) for the various insulator applications began with reactors built in 1961 and continued for the duration of the reactor test program.

While the choice of PyG as the insulating material was probably optimal from the standpoint of high-temperature thermophysical properties, neutronics, weight, cost, and ease of fabrication and machining, the PyG had major

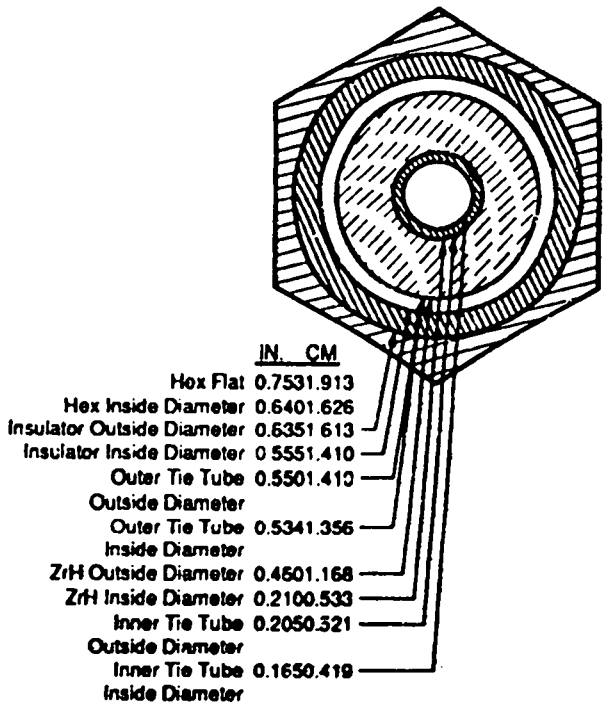

Fig. 1a. Nuclear engine reactor tie tube and support element geometry.

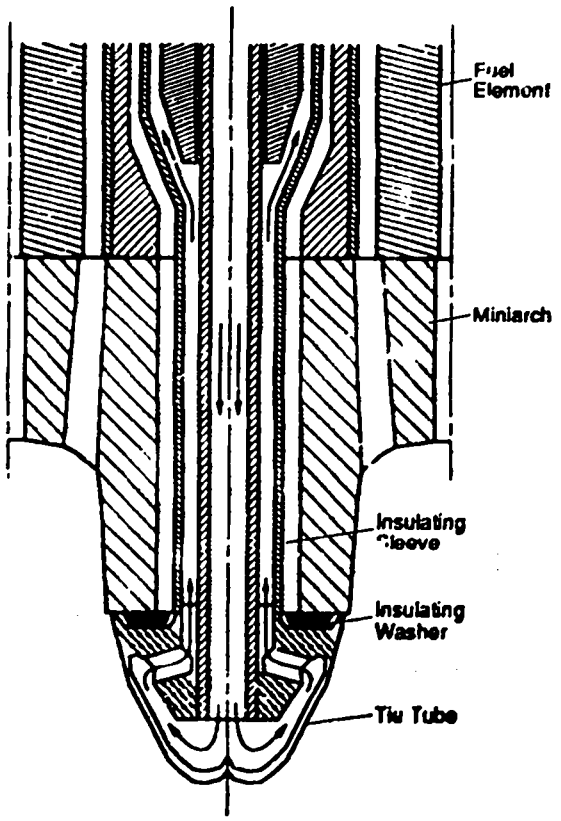

Fig. 1b. Hot-end-support axial section.

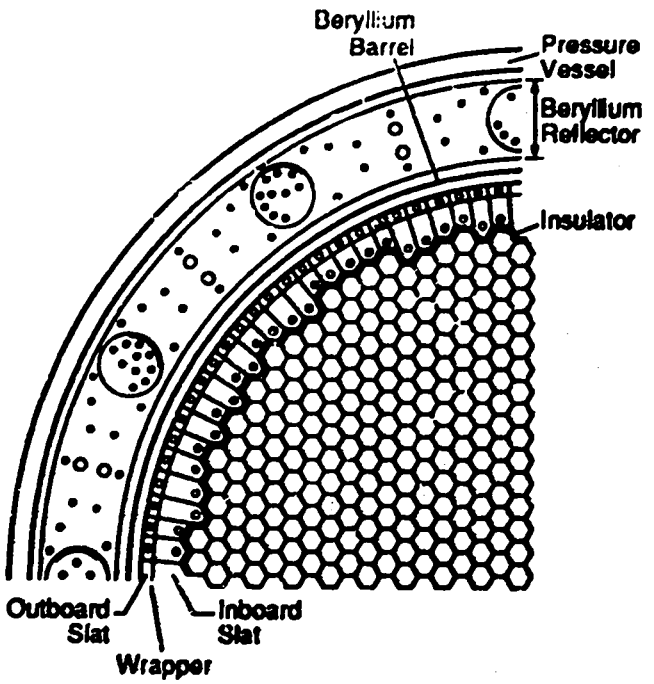

Fig. 1c. Reactor-core cross section.

flaws for the space reactor application. The major problem is corrosion. The PyG reacts chemically with the hydrogen propellant at high temperatures as follows:

$$xC + \frac{y}{2} H_2 = C_x H_y .$$

Thus, as the reactor continues to operate, the carbon is removed from the insulating PyG and is either redeposited at another part of the reactor or exits with the propellant as a gas. In addition, at sufficiently high temperatures, the layered PyG structure undergoes a change in which the ultimate result is the structure of polycrystalline, isotropic graphite. This is energetically the most stable form of graphite and predictably is found in nature. Thus, the reactor operating lifetime was limited by the length of time that the PyG could maintain its integrity and fulfill its insulating function. When this no longer happened, the lower temperature materials that had been insulated from the high-temperature reactor parts could not withstand the high temperatures and would melt or creep, presaging ultimate destruction of the reactor (this never actually happened).

To mitigate the insulator corrosion problem, the Rover Program investigators sought an insulating material that would be structurally stable, neutronically acceptable, and chemically inert in the reactor environment. The material of choice was zirconium carbide, which fulfilled many of the material requirements but is not an insulator. The successful research program to alter this material to allow it to be used as an insulator is described in this summary.

II. PYROLYTIC GRAPHITE

A. Structure and Properties

Pyrolytic graphite (also called pyrographite, pyrocarbon, PyG, or PyC) is graphite fabricated as a layered structure that gives it unique thermophysical properties. To understand this, it is important to understand the structure and how it influences the properties. Figures 2 and 3 show the structures of an idealized crystal of pyrolytic graphite. Figure 2 shows the structure viewed perpendicular to the layer planes. The planes are composed of carbon atoms in a two-dimensional set of hexagons with the carbon atoms at the apex of the hexagons, as shown in Fig. 2, by the solid line (a). The plane above (a) is displaced as shown in Fig. 2 by the dotted line (b). The next plane above is positioned directly above (a), the next above (b), and so on. This is called an (ab) stacking order. Figure 3 shows an angled view of the same structure with some key dimensions included. In Fig. 3 we can also more easily see the difference between the in-plane carbon-to-carbon distance (1.42 Å) and the inter-planar (this is labelled the "c" direction) distance (3.35 Å). These differences in dimensions give rise to the very anisotropic behavior of PyG. Because of the closeness of the carbon atoms in the "ab" direction, the interattractive forces and the lattice and electron field coupling are stronger than they are between the more distant planes in the "c" direction. Because of the relatively large distance between the planes, heat flow (which is related to the lattice and electronic coupling) in the "c" direction is greatly reduced compared to the "ab" direction. Thermal conductivities in the "c" direction have been measured at 1/200th of the value in the "ab" direction.[1] Similarly the decrease in interatomic force between the planes makes for a thermal expansion in the "c" direction about 10 times greater than that in the "ab" direction. Other properties are similarly affected. Taylor reported the thermal conductivity for PyG at room temperature to be 4-8 W/mK making it one of the better thermal insulators known.[1] The fact that the thermal conductivity doesn't change by a large factor at reactor operating temperatures (2273 K or greater) would make PyG an almost ideal choice for a Rover insulator if the structure and the hydrogen corrosion could be controlled. There are two caveats to this statement relating to the use of the PyG at temperatures above approximately 2273 K. The idealized crystal structure that has formed the basis for this discussion will transform into an isotropic, polycrystalline system if unconstrained and kept at high temperature for a sufficiently long time. This polycrystalline graphite commonly forms rapidly at temperatures in the vicinity of 3000 K; however, it has been observed to form at much lower temperatures (2000 K), but because the transformation rate is an exponential function of the temperature, the polycrystalline transformation can take a long time at the lower temperature. It is difficult to assign quantitative rates to this process because there are other influences on the crystallization process.

B. Improving the Structure of Pyrographite

Under the correct circumstances, the nature of the PyG structure may be improved by high-temperature treatment as can be noted from the following excerpt from an August 1965 Rover Progress Report. (This work was done at about 2973 K).

> Simultaneous application of compression and torsion at high temperatures has converted a continuously-nucleated pyrolytic graphite, having a well-developed fine cone structure, into a highly-ordered graphite having essentially the interlayer spacing of an ideal single crystal and very high degree of order in the orientation of layer planes. Periodic rotational disorientations, however, at intervals of about 500 to 1000 Å, have not so far been eliminated, and means of producing large single crystals from this pyrographite have not yet been developed.[2]

Similar studies were done by Ubbelohde in the 1960s in which the heat-treated PyG, compressed in the "c" direction, yielded very nearly perfect crystals. Without these artificial constraints, however, the PyG will appreciably

transform to the polycrystalline form at the temperatures at which the reactor was designed to operate (2673 K and up) to the detriment of the desirable thermophysical properties.

The other caveat has to do with the hydrogen corrosion. The rate of the reaction of the hydrogen with the graphite is exponential with temperature. An extremely rough rule of thumb is a doubling of the reaction rate for every 10 K rise in temperature. Appreciable corrosion was observed on some Rover test materials at 2223 K (see Part II.D. of this summary). It is clear that a relatively small increase

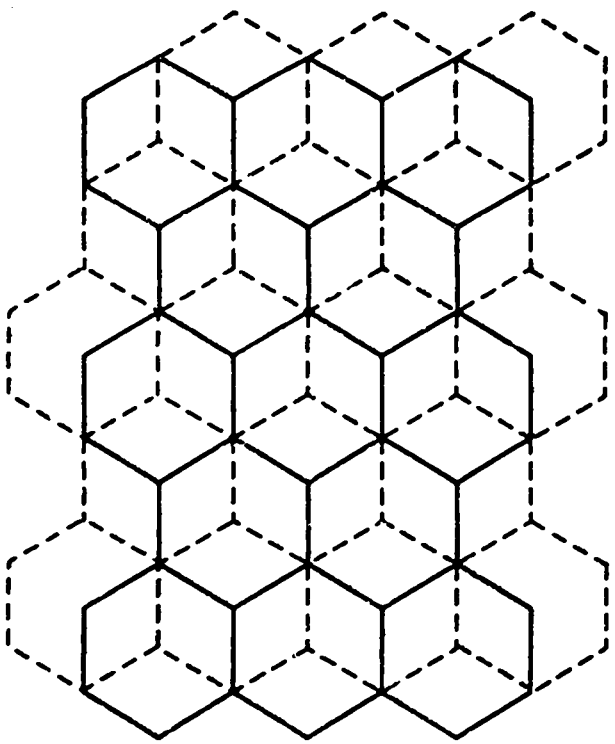

Fig. 2. Stacked planar structure of graphite viewed perpendicular to the ab planes. Solid lines (—) are the "a" layer, while dashed lines (- - -) are the "b" layer.

in operating temperature could have an enormous effect on the corrosion rate of the insulators with a concommittant decrease in the reactor's operating lifetime. It was largely because of these problems and potential problems that the Rover program embarked, in the 1960s, on an intensive study to identify insulator materials that would retain their structural integrity and resist any corrosive attacks under the reactor environment under optimized temperature and flow conditions.

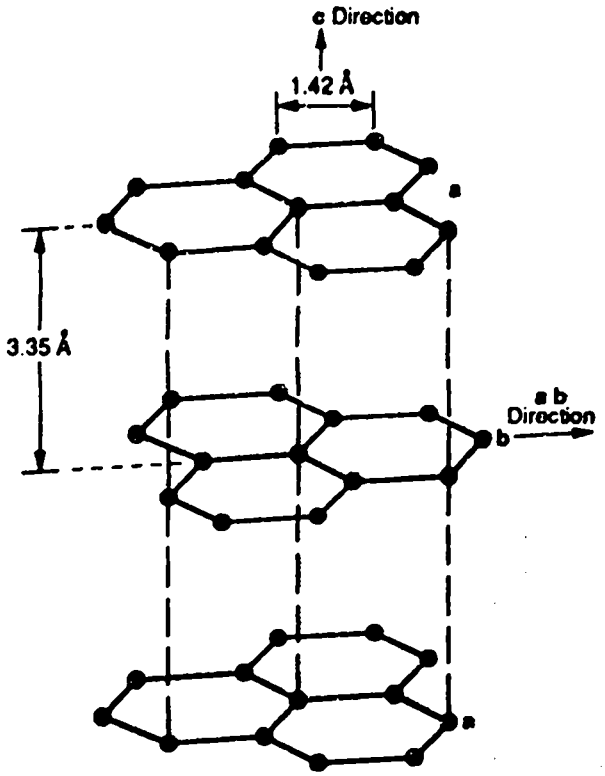

Fig. 3. Graphite crystal structure.

Pyrolytic graphite is fabricated by allowing a hydrocarbon gas (e.g. methane, ethane, or ethylene) to decompose at elevated temperatures (pyrolysis) and having the carbon deposit on a cooled pre-shaped substrate. By appropriate choice of gas, pressure, temperature, etc., the structure and the shape of the vapor-deposited artifact could be controlled. While ideal crystals, like that shown in Fig. 3, are not necessarily formed during the chemical vapor deposition (CVD) without further treatment, the properties of PyG made in this manner for commercial purposes are closer to the crystal properties than they are to those of the more common polycystalline-electrode graphites made by either extrusion or by hot pressing and as such were quite useable for the Rover reactor applications.

Attempts to clad the PyG to prevent hydrogen corrosion were largely unsuccessful. Corrosion- and ablation-resistant carbonaceous materials that were developed for the U.S. space program probably have better corrosion resistance than the PyG we have described; however, the corrosion resistance comes at the expense of some of the more desirable properties of the PyG, such as the low thermal conductivity. It is to be noted however, that other carbonaceous materials may become important in future high-temperature reactors if some of the severe dimensional restrictions in the Rover designs are relaxed.

C. Experience with PyG in the Rover Program

Because of the large number of confusing units commonly used to report heat flow, Table I is included to show the relationship between various systems of units. The commercially procured PyG used in the Rover program had "c" direction thermal conductivities comparable to the values reported for the idealized materials already described. As an example, Table II (taken from a May 1969 Progress Report[3]) records thermal conductivities measured in the radial (i.e. "c") direction on PyG tubes made for Rover. The values are comparable to those reported by Taylor.[1] The thermal conductivities are similar because of offsetting influences from the crystal structure and interplanar cracks that form when the tubes are cooled from the fabrication temperature (which is in excess of 1000 K). While the crystal structure is not ideal, tending to increase the thermal conductivity in the "c" direction, the crack formation balances the increase. The cracks tend to decrease the thermal conductivity at temperatures below about 1500 K. Other influences from impurities and mechanical flaws in the material cannot be evaluated at this time, but experience suggests strongly that these influences would be much less pronounced than those observed. In retrospect, more careful and direct control of the quality of the structural and physical character of the manufactured artifacts (something that would be far easier to do now with the tools available to us in the 1990s) could yield a product better fitted to the ultimate application.

A departure from ideality is also noted in the measurements of thermal expansion reported in August 1969.

D. Properties of PyG

Thermal Expansion of PyG Tubes. The thermal expansion of PG tubes, 0.633-in. o.d. by 1.71-in. long by 0.040-in. thick, was measured. The longitudinal expansion was 1.86×10^{-6}/°C and the transverse expansion was 2.40×10^{-6}/°C from 20 to 1750°C [293 to 2023 K]. These tubes were similar to those used in Pewee 1 support elements and to those to be used in Pewee 2 support elements.

Here, instead of a "c" to "a" (i.e., "transverse" to "longitudinal") thermal expansion ratio of about 10, as expected for the idealized material, the ratio is about 1.3. This is probably caused by a combination of crystal imperfections and partial exfoliation of the layer planes in the tubes used for the measurement. The cracking between the planes in the tubes (already described) decreases the measured thermal expansion in the "c" direction as well as the thermal conductivity. This was indeed observed in the tubes and the explanation was supported by the relatively low densities that were observed. Effects of impurities and mechanical flaws are minimal for this type of measurement of averaged thermal expansion. Again, if it is important that the properties of the artifact be closer to ideal, direct control of the crystal structure (and in the case of the tubes or other special shapes, the physical structure) will be crucial to that attempt.

The reactions between hydrogen and carbon have been known and reported in the open literature for many years. This was manifested in the Rover experience by corrosion of PyG by hydrogen coolant. Most of the studies reported

Table I. Conversion Factors for Thermal Conductivity

To Go From ↓ / To → (Multiply By ↘)	$\frac{W}{m\,K}$	$\frac{W}{cm\,K}$	$\frac{cal}{cm\,s\,K}$	$\frac{kcal}{m\,h\,°F}$	$\frac{Btu}{ft\,h\,°F}$	$\frac{Btu\,in.}{ft^2\,h\,°F}$
1 $\frac{J\,m}{m^2\,s\,°C}$ or $\frac{W}{m\,K}$	1	1×10^{-2}	2.388×10^{-3}	0.8598	0.5778	6.933
1 $\frac{J\,m}{cm^2\,s\,°C}$ or $\frac{W}{cm\,K}$	1×10^{2}	1	0.2388	85.98	57.78	693.3
1 $\frac{cal\,cm}{cm^2\,s\,°C}$ or $\frac{cal}{cm\,s\,K}$	418.68	4.1868	1	360	241.9	2903
1 $\frac{kcal\,cm}{m^2\,h\,°F}$ or $\frac{kcal}{m\,h\,°F}$	1.163	1.163×10^{-2}	2.778×10^{-3}	1	0.6720	8.064
1 $\frac{Btu\,ft}{ft^2\,h\,°F}$ or $\frac{Btu}{ft\,h\,°F}$	1.731	1.731×10^{-2}	4.134×10^{-3}	1.488	1	12
1 $\frac{Btu\,in.}{ft^2\,h\,°F}$	0.1442	1.442×10^{-3}	3.445×10^{-4}	0.124	8.333×10^{-2}	1

an accelerated corrosion and attack at the edges of the PyG in the "ab" direction. The implication is that the carbon atoms at the edges of the carbon planes are more reactive than those in the plane. A reasonable approach to controlling the corrosion problem is to allow the layer planes to wrap around the edges of an artifact thus presenting only a "c" direction to the hydrogen corrosion. This was considered and reported in August of 1969 and is quoted below.

> **Hydrogen Corrosion of Specially Oriented Pyrographite.** Hot gas tests were performed to determine the corrosion resistance of pyrolytic graphite which had been formed into shapes intended to test the corrosion resistance of pyrographite in the "c" direction. One type resembled the button of a mushroom and the other a shear pin completely overcoated with pyrographite. Corrosion was not entirely uniform, but attack seemed [to] occur more rapidly on one area than on another. Exposure of 3 min to H_2 at 4500°R [2500 K]often removed carbon to a depth of ~ 100 mils or more. It is clear that pyrographite is vulnerable to H_2 corrosion in the "c" direction at all temperatures above 4000°R [2222 K].[4]

In an effort to blend the desirable high-temperature integrity and corrosion properties of ZrC with the excellent thermophysical properties of the PyG, ZrC-PyG composites were prepared and thermal diffusivities of the alloys measured. (Note: the thermal conductivity is the product of the thermal diffusivity, density, and heat capacity. To a first approximation, the trend in thermal diffusivity is the same as the trend in thermal conductivity.) The results of these measurements were reported in August of 1968 and are reproduced here.

> **Thermal Diffusivity of ZrC-PyC Composites.** The thermal diffusivity of four ZrC-pyrolytic graphite (PyC) composites, prepared by simultaneous deposition by [The] Raytheon [Co.], was measured from 800 to 2100°C [1073 to 2373 K] by the laser flash technique. The composites contained 15, 50, 70, and 80 wt % ZrC, respectively. The thermal diffusivity values vs composition at 1000, 1500, and 2000°C [1273, 1773, and 2273 K] are plotted on a semilogarithmic scale [see Fig. 4].
>
> There is an exponential relationship between the thermal diffusivity, α, and the wt % ZrC in the ZrC-PyC composite, and $k = 0.0036$ cm²/sec.[5]

E. Summary and Recommendations for Future Use

Overall, we learned some lessons. The assumption that properties of PyG could be controlled by specifying processing conditions was certainly well founded, but hardly sufficient. As we commented earlier, with the vast variety of analytical techniques available today (1991), specifications that spell out the required structural, physical, and chemical parameters may be monitored directly on production runs of PyG, thus allowing these materials to more closely match the engineering specifications (see Table III).

III. ZrC BASED INSULATORS

A. Overview

It was recognized early in the Rover program that any materials chosen for use in the high-temperature region of the reactor would have to resist hydrogen corrosion and radiation damage and maintain their integrity while not interfering with the reactivity and the control functions in the reactor. In the earliest days of the program, R. Schreiber (the Division leader) and I discussed the desirability of finding that most-important, all-purpose material with no negative characteristics, "impervium," that we both remembered from the Buck Rogers fantasies of the 1930s. If we could have legislated the materials for the program rather than been forced to use what nature willed to us, we would have done it. Having no other option, it became the job of the Rover management to pursue research and development on materials that offered the most tenable set of compromises for the job to be done. It was recognized in the 1950s that the most promising material would be a

Table II. Thermal Conductivity of PyG Sleeves

Gaseous Environment	Temperature (K)	Thermal Conductivity $(W/cm\,K) \times 10^{-3}$	Temperature (K)	Thermal Conductivity $(W/cm\,K) \times 10^{-3}$
Hydrogen	1366	10.4 (upper limit)	1921	11.4 (upper limit)
Helium	1366	8.5–10.1	1921	10.1–11.1
Nitrogen	1366	6.6–7.2	1921	8.1–8.6
Vacuum	1366	2.7–4.9	1921	4.8–6.3

refractory zirconium compound, probably an oxide or a carbide. This was hardly startling in view of the country's power reactor experience, but even that experience had little to offer in terms of direct technology transfer. Rover's demands exceeded all engineering practice. For these reasons, an ever-accelerating, in-depth research program was initiated as the limit of usefulness of the PyG systems was approached in the 1960s.

Figure 5 shows the areas of concentration and how they finally culminated in the vigorous and successful development of porous, sub-stoichiometric zirconium carbide insulators.

B. ZrO_2-ZrC

Development of the ZrC and the ZrC-ZrO_2 composite materials was spurred by the desire to replace the PyG in the Pewee reactors, especially inside the beryllium reflector at the core periphery (see Fig. 1c). Various composites were made by hot pressing the materials at 2073 K and 6400 psi. Measurements of thermal conductivity at room temperature are shown in Table IV (reported 11/69).[6]

Additional research yielded thermal conductivity measurements on materials exposed to various temperatures up to 2773 K (see Table V).

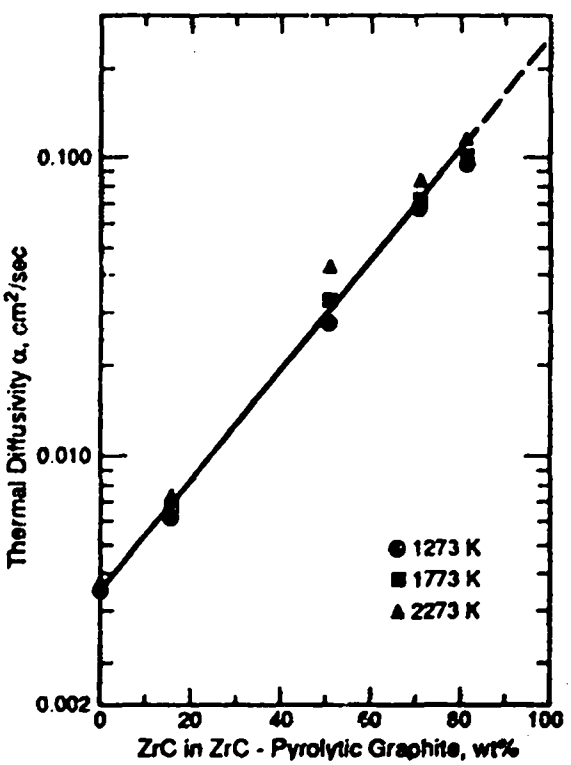

Fig. 4. Thermal diffusivity of ZrC-PyC composites.

Analysis of heat transfer in the Pewee 2 reactor using these composites showed that the composite, while effective, was far from the requirements specified in the engineering design. This is illustrated in Fig. 6.

Measurements were also made to demonstrate the viability of the concept of increasing the porosity of the insulator materials to decrease the thermal conductivity. Measurements of this genre on ZrC at room temperature are reproduced in Table VI.

The influence of added porosity on the insulators introduced another dimension to the use of these ceramic materials because changes in density affected strengths, creep properties, moduli, and potential operating characteristics of the reactor.

Once the decision was made to operate Pewee 3 with a core temperature of 2573 K or greater, the use of ZrO_2-ZrC composites was ruled out and in late 1970 the composites were dropped from consideration as peripheral insulators. It was decided that ZrC or a ZrC-C composite in some form would be more appropriate for future research.

C. ZrC-C

Experiments were also performed with ZrC-C to examine its viability as an insulator. In August 1970, ZrC-C extrusions with about 5 wt % free carbon were reported. Initial measurements of these materials revealed that the thermal conductivity was substantially greater than that of hot-pressed ZrC. The samples were then heat treated in hot hydrogen and the thermal conductivities remeasured with the result that as the free carbon was removed by this treatment, the thermal conductivity was reduced. These data are reproduced in Table VII.

The conclusion was reached that ZrC would be a better insulating material if it contained no free carbon. Further experiments then concentrated on ZrC.

D. ZrC

The research on ZrC started in earnest in 1971. Initially there were investigations of the various thermal, physical, and mechanical properties of ZrC made at near theoretical density and with deliberately introduced porosity. While these efforts were not definitive, it was at about this time that discussions about the best way to measure the thermal conductivity (an area of uncertainty at the time) of the experimental insulator materials began to converge and the flash diffusivity method was adopted as the standard.[7] We obtained a thesis written in one of the Max Planck Institutes (Stuttgart) which when translated led us toward looking carefully at substoichiometric ZrC made with vacancies in the carbon lattice because this alone was most effective in decreasing the thermal conductivity. This new information, combined with the fabrication of

Table III. Measured Properties of PyG Produced for the Rover Program Compared with Literature Data for More Nearly Ideal PyG

PyG	Density (g/cm^3)	Thermal Conductivity (W/mK)		Thermal Expansion (cm/cmK)	
		"c"	"ab"	"c"	"ab"
Rover	1.7–1.95	1–5	not done	26	20
Ideal	1.9–2.05	4–8	800–1600	100	10

Table IV. Thermal Conductivity Data

Composition	Density g/cm^3	Density % Theor.	Thermal Conductivity $(W/cm\ K)$
ZrO_2			0.017
75 vol % ZrO_2 25 vol % ZrC*	4.970	--	0.018 to 0.023
75 vol % ZrO_2 25 vol % ZrC**	5.394	93.91	0.0155
50 vol % ZrO_2 50 vol % ZrC**	5.487	90.24	0.026
25 vol % ZrO_2 75 vol % ZrC**	5.362	92.60	0.035
ZrC			0.273

*CaO-stabilized ZrO_2
**Unstabilized ZrO_2

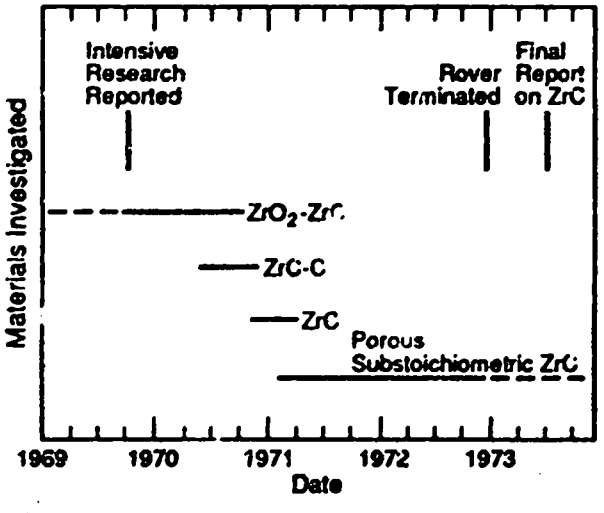

Fig. 5. Materials investigated during the Rover insulators program: 1969–1973.

porous materials with the substoichiometric ZrC_x (as it came to be known), led to a series of experiments and a redirected research and development program that had every indication of yielding a successful insulator material. Unfortunately, as this was coming to closure, the Rover program was terminated and all work in this area ceased.

E. Porous Substoichiometric ZrC_x Insulators

Fortunately, a comprehensive and timely report on this effort was written and published at Los Alamos. This report, LA-5224, "Research, Development, and Production of Substoichiometric Zirconium Carbide for High-Temperature Insulation," (July 1973), written by Paul Wagner, is the final portion of this report on Rover insulators.

Table V. Effect of Time and Temperature on Hot Pressed 75:25 Vol % ZrO_2-ZrC_x Composites

Exposure Temperature (K)	Time at Temperature (h)	Room Temp. Thermal Conductivity ($W/_{cm\ K}$)	Room Temperature Density ($g/_{cm^3}$)	Microstructure
2073	0	0.022	-	Specimens exposed for up to 8 h showed little change. Exposure in flowing H_2 for 8-16 h showed formation of substoichiometric ZrC.
	1	0.011	-	
2573	0	0.020	5.52	Sample showed some formation of substoichiometric ZrC but there was no evidence of melting or dimensional changes.
	1	0.015	5.29	
	2	0.0145	5.20	
	4	0.0198	5.09	
	8	0.0124	5.24	
	16	0.024	5.26	
2773	0	0.022	-	Formed some substoichiometric ZrC. Pronounced evidence of melting with increased time at temperature.
	1	0.0155	-	
	2	0.011	-	
	8	0.0072	-	

The samples treated at 2073 K showed a drop in conductivity from 0.022 to 0.011 W/cm K after 1 h suggesting the possibility of a chemical reaction taking place. The sample treated at 2073 K for 16 h gave a value of 0.019 W/cm K which was approaching that of the as-hot-pressed material. Metallographic examination showed what appeared to be increased migration of ZrC into the ZrO_2 with increasing time and temperature. There was no evidence of a skin or surface reaction on these samples.

Table VI. Effect of Density on Thermal Conductivity of ZrC

Density		Thermal Conductivity
(g/cm^3)	(%theoretical)	(W/cmK)
6.43	97.3	0.243
6.18	93.5	0.119
4.48	67.8	0.077
4.30	65.1	0.0428
4.08	61.7	0.0278

Table VII Thermal Conductivity of Extruded, Low-Density ZrC Before and After Hydrogen Leaching[a]

Temperature (K)	Calculated Thermal Conductivity, (W/cmK)				
			Extruded, Low-Density ZrC		
	Hot-Pressed ZrC 95% theor. dens.	ATJ-S Graphite	As Received 71.7% theor. dens.	H_2-Leached 67.2% theor. dens.	Leach + 1 hr at 2498 K 65.8% theor. dens.
300	0.20	1.51	0.43	0.05	0.09
500	0.21	1.27	0.38	0.06	0.11
1000	0.23	0.71	0.28	0.07	0.12
1500	0.28	0.53	0.25	0.08	0.13
2000	0.32	0.45	0.23	0.11	0.15
2400	0.36	0.41	0.23	0.15	0.17

[a]Heat flux measured ⊥ to extrusion direction, i.e., across grain.

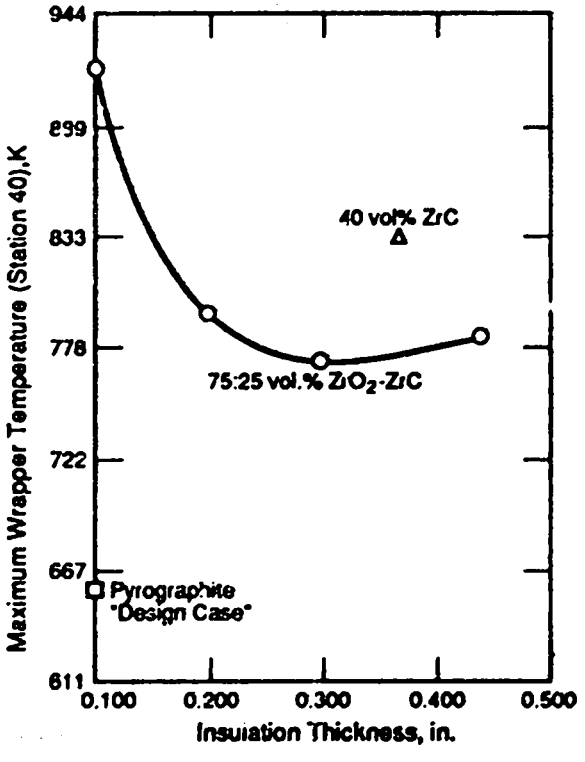

Fig. 6. Predicted performance of prospective insulation materials in Pewee 2 core periphery.

References

1. R. Taylor, "An Investigation of the Heat Pulse Method for Measuring Thermal Diffusivity," *British Journal of Applied Physics* 16, 509-515, 1965.

2. "Quarterly Status Report of LASL Rover Program for Period Ending August 31, 1965," Los Scientific Laboratory report LA-3398-MS (October 1965).

3. "Quarterly Status Report of LASL Rover Program for Period Ending May 31, 1969," Los Alamos Scientific Laboratory report LA-4203-MS (June 1969).

4. "Quarterly Status Report of the LASL Rover Program for Period Ending August 31, 1966," Los Alamos Scientific Laboratory repon LA-3598-MS (September 1966).

5. "Quarterly Status Repcrt of LASL Rover Program for Period Ending August 31, 1968," Los Alamos Scientific Laboratory report LA-4012-MS (October 1968).

6. "Quarterly Status Report of LASL Rover Program for Period Ending November 30, 1969," Los Alamos Scientific Laboratory report LA-4344-MS (December 1969).

Research, Development, and Production of Substoichiometric Zirconium Carbide for High-Temperature Insulation

LA-5224

originally published in July 1973

Editor's note:

The following is a reprint of a Los Alamos Scientific Laboratory report. It has been photographed from an original copy, with only the page numbers altered to fit with this report. The tables and figures retain their original numbering and sequence and hence are numbered separately from the first 10 pages of text.

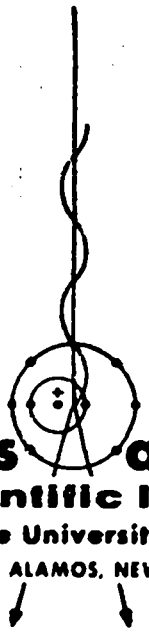

LA-5224
UC-25 and UC-80
ISSUED: July 1973

Research, Development, and Production of Substoichiometric Zirconium Carbide for High-Temperature Insulation

by

Paul Wagner

This work was done as a support effort in the Rover project.

CONTENTS

RESEARCH, DEVELOPMENT, AND PRODUCTION OF SUBSTOICHIOMETRIC ZIRCONIUM CARBIDE FOR HIGH-TEMPERATURE INSULATION

by

Paul Wagner

ABSTRACT

Zirconium carbide is a chemically stable, high-melting material uniquely suited to reactor applications. This report describes the research, development, fabrication, and evaluation of porous ZrC as an insulator intended for use in the high-temperature, gas-cooled Rover reactors. ZrC_x is a stable, single-phase carbide in the $0.98 \geq x \geq 0.59$ region. The thermal conductivity of ZrC_x is very sensitive to the vacancy concentration in the carbon sublattice (1-x). To decrease sufficiently the thermal-conductivity value of ZrC_x to make the insulator, the carbon-zirconium ratio was decreased to an optimum value and the thermal conductivity was decreased further by introducing porosity in the ZrC_x matrix. By these techniques, the thermal conductivity of ZrC_x at 300 K was decreased from 50 $W m^{-1} K^{-1}$ to less than 1 $W m^{-1} K^{-1}$. Forty and seventy percent porosity ZrC_x were investigated and their properties were measured. The production material was a 70% porous fiber-based ZrC_x having satisfactory strength, thermal stress resistance, insulating power, and uniformity.

INTRODUCTION

As the Los Alamos Scientific Laboratory's (LASL) gas-cooled Rover reactor program progressed, reactor designs utilizing higher temperatures and longer use times evolved. Early designs employed pyrolytic graphite to insulate the thermally hot fuel elements from the cooler reactor components. Because pyrolytic graphite reacted with the hot hydrogen environment, reactor lifetimes were limited by the corrosion of the insulators. Interest was focused on the substoichiometric monocarbide of zirconium (ZrC_x) as the more chemically stable insulator. Fabrication development on this material resulted in an end product that was a satisfactory insulator; also, an insulator system was generated where trade-offs could be made on the thermal conductivity, strength, and density of the ZrC_x. However, because of the structural nature of the ZrC fiber insulators, they were not wholly interdependent. It was possible to hold the density constant and yet to vary the strength and conductivity. With this kind of flexibility, the ZrC_x system can be tailored to a set of specifications in conductivity, strength, density, or related properties unique in refractory materials.

Of the various materials considered for the insulator, the carbides in the elements of groups 4a and 5a are the most attractive; all of which exhibit high melting points, chemical inertness in reducing atmospheres, and a spectrum of neutronic properties. Zirconium carbide was chosen because it has the lowest neutron capture cross section but it still retains the desired refractory qualities.

Using ZrC to insulate the hot fuel elements has one major drawback: in its theoretically dense state, ZrC is not an insulator. The thermal conductivity (λ) of ZrC is about 50 $W m^{-1} K^{-1}$ at 300 K, whereas an effective insulator should have a λ in the vicinity of 1 $W m^{-1} K^{-1}$ or less. Thus, developing a ZrC insulator for the Rover reactors was reduced to a fabrication program wherein the prime figure of merit, the thermal conductivity, was to be minimized. This was done by combining several methods. First an understanding of the effects of stoichiometry on

ZrC_x properties was gained. Then, by using an optimized C/Zr ratio, porous artifacts were manufactured with the intent of increasing the tortuosity of the heat-flow path and of increasing the thermal resistance. Of the several techniques employed in the fabrication investigations, the most successful was converting carbon fibers directly to ZrC by reaction with $ZrCl_4$. When the Rover project was terminated, insulator units of pure ZrC_x with thermal conductivities less than 1 $W\,m^{-1}\,K^{-1}$ were being fabricated on a routine schedule.

Our investigations were complicated by the uncertainty of whether or not λ measurements could be made accurately on the very porous materials. For this reason, various aspects of thermal-conductivity measurements and analyses are an essential part of the insulator development.

II. PROPERTIES OF SUBSTOICHIOMETRIC ZrC

The first step in the ZrC insulator development was to define the effects of structure of the substoichiometric ZrC_x on the thermal-conductivity and associated properties. Some work had been done in this area;[1] however, large gaps existed in the available information. We made an effort to generate self-consistent information that would demonstrate unambiguously the dependence of the thermal conductivity on the ZrC_x structure in the monophase region ($0.98 > x > 0.59$). Similar work was done with NbC_x partly because NbC_x has many of the properties that make ZrC_x so attractive and partly to aid in interpreting the ZrC_x results.

These researches consisted of a group of measurements done on carefully made and characterized samples of single-phase ZrC_x. Details of the methods used for sample preparation, sample characterization, thermal-diffusivity measurements, density determinations, porosity corrections (for nearly theoretically dense samples), heat capacity estimation, electrical resistivity measurements, and impurity influences are given in Appendix A.

The data on the effect of C/Zr atom ratio on λ at 300 K are summarized in Fig. 1. The crystal structure of both ZrC and NbC are of the rock-salt type (type B 1, face-centered cubic). The metal and the carbon atoms form interlocking face-centered cubic sublattices. The zirconium sublattice is stable only when all the lattice sites are occupied, but the ZrC_x is stable when there are vacancies in the carbon sublattice and when the substoichiometric carbide is formed. The change in λ shown in Fig. 1 was caused by an increase in the vacancy concentration in the carbon sublattice; the effect of impurities such as oxygen, nitrogen, and sulfur is minimal (for details see Appendix A). A similar dependence of λ on the carbon-to-metal ratio was observed in NbC.

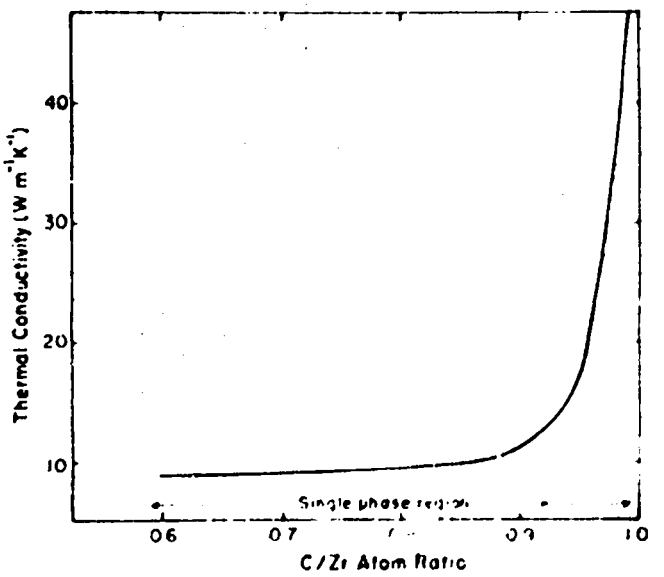

Fig. 1.
Effect of stoichiometry on thermal conductivity in ZrC_x.

The data in Fig. 1 and the electrical resistivity measurements made at 300 K on these samples show that about 37% of the thermal energy is carried by electrons and the other 63% is carried by lattice waves (phonons). If one estimates that, based on the pure material, a 1% increase in the vacancy concentration doubles the electrical resistivity (observed for a variety of metals such as copper, zinc, and aluminum) and if the phonon scattering is proportional to the square root of the defect concentration,[2] then the very sharp dependence of λ on C/Zr is understandable. The electronic component of the thermal conductivity is related to the electrical resistivity by

$$\lambda_{\text{electronic}} = \frac{LT}{\rho_R} ,$$

where T = temperature; ρ_R = resistivity, ohm m; and L = Lorenz function, $2.45 \times 10^{-8}\ V^2\ K^{-2}$. For C/Zr = 0.9, that is, for a vacancy concentration of 10% in the carbon sublattice, the above-type calculation predicts a $\lambda = 12\ W\,m^{-1}\,K^{-1}$, which is very close to the value shown in Fig. 1. The behavior of the thermal conductivity with temperature is also consistent with this mechanism. The high-temperature measurements reported in Refs. 3 and 4 show a monotonic increase in λ with temperature. Because these measurements are made at temperatures that exceed the Debye temperature, the phonon contribution will decrease as the reciprocal of the absolute temperature, but the behavior of the electrical resistivity indicates that a simultaneous filling of the conduction

band occurs with sufficient magnitude to cause a net increase in λ. This increase was confirmed by observations made at LASL[5] where the electronic component of the total thermal conductivity increased to about 75% at temperatures above 1500 K.

NbC acts similarly to ZrC despite the difference in the band structure of the two materials. This is a powerful indication that the mechanistic description of the behavior of the conductivity is realistic.

Russian data[6] indicate that the linear coefficient thermal expansion (CTE) is nearly constant with stoichiometry. The following CTEs were reported.

Composition	CTE (K^{-1})
$ZrC_{1.0}$	6.57×10^{-6}
$ZrC_{0.90}$	6.62×10^{-6}
$ZrC_{0.80}$	6.66×10^{-6}
$ZrC_{0.75}$	6.70×10^{-6}
$ZrC_{0.65}$	6.75×10^{-6}

Note. CTE averaged from 300 K to 1273 K.

III. FABRICATION METHODS FOR POROUS ZrC

Several methods were used to manufacture porous ZrC during the development program. These methods are indicated in Table I. In addition to the methods listed in Table I, fabric, papers, carbonized bodies, and extruded carbons and graphites can also be converted into porous ZrC. A combination of these methods can also be used. The table gives those methods that proved most promising for the Rover applications.

Hot-pressing techniques may be applied by using pure ZrC at sufficiently elevated temperatures and pressures. To achieve desired porosities, most of the hot-pressing work was done with mixtures of ZrC, ZrO_2, carbon in some form, and a variety of pore-formers, such as Teflon. Excess carbon was removed by reaction with hot hydrogen (leaching). There is an endless variety of raw materials from which porous ZrC can be made by using this technique. The final product is strong and the porosity may be controlled by a combination of the material formulation and the pressing pressures. One Westinghouse Astronuclear Laboratory ZrC made by this method had P = 55%, $\lambda = 2\ W\ m^{-1}K^{-1}$, σ = 13.8 MPa and E = 13.8 GPa. This hot-pressing method was used to fabricate parts used in LASL's Nuclear Furnace No. 2 (NF-2); however, specifications other than thermal conductivity had to be met for this application.

The fiber impregnation method used by the McDonnell Douglas Astronautics Company under contract to the National Space Technology Laboratories and Space Administration (Contract No. SNPC-67) is this method, woven fiber made of carbon or of carbon precursor materials was soaked in a $Zr(NO_3)_4$ solution, which formed ZrC when heated. This process could be repeated as often as desired to build the density up to the desired value. Measurements of λ on these materials are reported to be as low as $0.5\ W\ m^{-1}K^{-1}$, however, LASL tests proved uncertain because relatively large amounts of residual carbon fibers were found to exist in the purported ZrC matrix. The technique is attractive because of the potential control of the geometric structure of the ZrC fibrous phase.

Direct reaction of carbon or graphite bodies with $ZrCl_4$ gas to yield ZrC was tried by using hollow carbon

TABLE I

FABRICATION METHODS FOR POROUS ZrC

Method	Porosity Range (%)	Minimum Thermal 300K Conductivity ($W\ m^{-1}K^{-1}$)	Comments
Hot-pressing	0-70	3.0	Strong
Extrusion	20-50	3.0	Strong
Fiber impregnation	15-60	0.5	Flexible technique
Carbospheres + $ZrCl_4$ gas	80	0.8	Slow process
Carbon foam + $ZrCl_4$ gas	80	5.0	Slow process
Carbon fibers + $ZrCl_4$ gas	65-90	0.4	Fast, flexible method

spheres (carbospheres) that were bonded together with a polyfurfural alcohol binder, using carbon foam and carbon fibers. The carbospheres and foams are relatively impermeable to the reacting gas and, as a consequence, the reaction times required for conversion are extremely long in comparison with those for the fiber systems. The interlocked spheres in the ZrC carbospheres created a strong material, and the point contacts between the spheres provided an effective thermal resistance for a λ (300 K) = 0.8 W m^{-1} K^{-1}. The carbon-foam system suffers from the same deficiencies as the carbospheres except that a high value of λ may be expected for a foam matrix. In particular, a trial test[8] of the 72% porous ZrC made from foam yielded λ (300 K) = 5 W m^{-1} K^{-1} or higher, the modulus of rupture was 10.5 MPa, the elastic modulus was 14.9 GPa, and the average strain to failure was about 0.07%. It took ten times longer to fabricate this material than it did to fabricate the carbon-fiber systems of the same mass.

The extrusion methods used for porous ZrC and the carbon fiber-gas conversion to ZrC were the most successful techniques employed. Both systems were important to the Rover insulator program and are discussed separately in this report.

IV. EXTRUDED POROUS ZrC

An extensive study was made on the fabrication and properties of extruded ZrC of approximately 40% porosity during the insulator development program. In general, this material was made by extruding a mixture of ZrC, ZrO_2, a polyfurfural alcohol (binder), carbon or graphite powder, and Teflon or nylon. This mixture was then sintered in helium or argon at 2773 K for 7.2 ks (2 h), excess carbon was removed by exposure to hydrogen at 2573 K for 28.8 ks. This gave a very high-strength material of about 60% theoretical density that was grey in appearance, was machineable, and was quite tractable. The results and details of the fabrication development effort on these materials is included in greater detail in Appendix B, and will not be discussed further here.

A. Thermal-Conductivity Measurements at 300 K

Although the thermal conductivity (λ) of the porous ZrC insulators was the prime figure of merit, disparities in early λ results and the uncertainty about whether or not transient methods could be successfully applied to systems of 40% void stimulated a vigorous effort to define the accuracy, the reproducibility (using a variety of methods), and the precision of the measurements. The first step was to assure the inherent accuracy of the equipment used—two flash-diffusivity systems, a contact probe system and a cut-bar steady-state apparatus. Standardization was done using Armco iron (which had been calibrated vs a sample of Round Robin Armco), pyroceram (Code 9606), and fired Lava A.[9] The second step was to have different investigators make λ measurements on the porous ZrC to assure that the introduction of the porosity did not influence adversely the reproducibility of the thermal-conductivity measurements. The third step was to make a relative measurement of λ for ZrC against well-known standards to assure that the results obtained by the flash method still retained the necessary degree of accuracy.

Three investigators measured the room temperature thermal conductivity, and thermal diffusivity of four ZrC extrusions.[10] Where possible, identical samples were used to obtain characteristic data for production materials (Lots 4558, 4575, 4706, 4742) and some statistics on the reproducibility of the measurements made by the different investigators. These data, compiled in Table II, show no disparity in measured results and show a data spread of less than 10% where identical samples were used. For one of the extrusions, the sample thickness was varied from 0.0202 m to 0.0383 m (a factor of 3.6 in influence in the diffusivity measurements because the thickness term is squared). Measurements were made in vacuum, argon (at 0.1 MPa and at 10 kPa), helium, and air and were corrected for the convective heat losses. All these data are shown in Table II. In general, there were no contradictions in the measurements. If samples of identical materials (but not identical samples) were used, variations in the investigators results could exceed the 10% precision demonstrated for the measurements. It is inferred from this that the variability in these materials from one point to another was greater than the uncertainty in the measurements.

The third step in verifying the methods used was to make a direct comparison of the results obtained by steady-state techniques with those obtained by transient methods on identical samples of the porous ZrC in question. The thermal conductivity of a 40% porous ZrC sample was measured near room temperature using an axial-flow, steady-state comparison. A detailed description of this apparatus is given in Ref. 9. These measurements were compared with those made by the flash-diffusivity method on samples used for the steady-state measurements.[11] The results of these investigations are summarized very briefly as follows.

TABLE II

COMPILATION OF THERMAL CONDUCTIVITIES OBTAINED AT LASL ON CONTROLLED SAMPLES OF 40% POROUS, EXTRUDED ZrC
ALL DATA IN $Wm^{-1} K^{-1}$ UNITS

Sample	Condition	Sibbitt's Results	Wagner's Results	Morrison's Results				
				Vacuum	Air	Helium	Argon	Argon[a]
4706	NF-1 production material. Leached	4.6 (2 det)	4.7	4.8	--	4.9	4.9	--
		4.4 (2 det)	4.9	4.7	4.7	4.8	--	--
		4.5 (2 det)	4.3	--	4.1	4.1	4.1	4.0
				4.3	4.6	4.4	--	4.4
				4.0	4.4	4.3	--	4.1
				4.3	4.3	4.3	--	4.4
4706	Leached	4.4 (2 det)	--	--	--	--	--	--
		4.7 (2 det)	--	--	--	--	--	--
		4.5 (2 det)	--	--	--	--	--	--
4558 Zr-1	Leached	3.7 mean	4.7	4.7	--	--	--	--
		4.9 max	4.8	4.8	--	--	--	--
		(9 det)	4.6	4.4	--	--	--	--
			4.4	--	--	--	--	--
4574 Zr-2	Leached	3.4 mean	3.7	3.7	--	--	--	--
		3.7 max	3.5	3.5	--	--	--	--
		(5 det)	3.4	3.7	--	--	--	--
			3.8	--	--	--	--	--
4742 Zr-1	Leached	4.2 mean	4.5	4.4	--	--	--	--
		4.5 max	4.6	4.6	--	--	--	--
		(8 det)	4.7	4.8	--	--	--	--
			4.8	--	--	--	--	--

[a] At 0.1 M Pa (1 atm)

NOTE: Underlined data indicate identical samples (horizontally).

Method	Sample Orientation	Temp (K)	Thermal Conductivity $Wm^{-1} K^{-1}$
Steady state	Parallel to extrusion axis	380	6.3
Transient (flash diffusivity)	Parallel to extrusion axis	295	6.2

The indeterminate error is estimated to be ~10% for the steady-state results and ~5% for the flash-diffusivity results.

It is clear from the preceding that the λ measurements reported here occupy a very high confidence level. Of the various techniques employed during this project, all but one gave accurate and self-consistent answers. The exception was the Colora method which gave self-consistent results, but the answers were invariably lower than all others.[11] The necessity for proving the validity of the measurements upon which [illegible] program is based cannot be over-emphasized.

B. Thermal-Conductivity Measurements at Elevated Temperatures

The questions concerning the validity of the λ measurements at 300 K also existed for measurements of 40%

porous ZrC materials at elevated temperatures. One of the first groups of experiments was performed to demonstrate the reproducibility of the change of the thermal conductivity with increasing temperature.[13] Samples from different extrusion lots, but with nominally similar properties, increased in λ as the temperature was increased from 300 to 2600 K. In vacuum, λ(2600 K)/λ(300 K) was approximately 2.75 for all the extruded materials studied. The reliability of the transient laser flash-diffusivity technique for elevated temperature measurements using porous ZrC was demonstrated by sending samples, measured at LASL by this method, to the Thermo-Physical Properties Measurement Facility, Sandia Laboratories (Albuquerque, NM), for the same type measurements. The LASL and Sandia results were in excellent agreement.[14] The final step in the experimental λ(T) program was to make measurements of λ(T) using a radial heat flow, steady-state measurement on the 40% porous ZrC. All these λ(T) results[5,14,15] are shown in Fig. 2. Figure 2 shows that although details from the steady-state measurements are not available below 1300 K, excluding λ(300 K), in regions of overlapping temperature there is little to choose between the results obtained from the flash-diffusivity measurements and those obtained from the steady-state experiments. The error-estimate bands shown in Fig. 2 imply that high-temperature results of λ measurements are very difficult to make with the same level of confidence as those reported for 300 K.

C. Modeling Porous ZrC

Originally, the insulator was to be used in an environment of high-pressure hydrogen, but because no facility existed for making λ(T) measurements in this environment, it was necessary to model the porous ZrC to calculate λ(T) for the reactor applications, if we postulate that the porous ZrC consists of three phases, one a continuous matrix of the ZrC, one a discontinuous phase (of fixed-bed), and one a void structure, it is possible to calculate some of the system properties. This was done for extrusion lot No. 4706 by utilizing published data for λ(T) of continuous ZrC[3,4] and predicting, from engineering principles, the conductivity of the fixed-bed phase. The void structure was postulated to be isometric and calculations were made for two pore sizes.[16] The results of these studies are summarized in Fig. 3. Here the calculated λ(T) is compared directly with the measured λ(T) for the same material as that used for the modeling. The agreement is quite good. Note the sharp upturn of the measured values compared with the calculated values for the thermal conductivity at higher temperatures. This is probably associated with the difficulty in characterizing the void geometry. A photomicrograph of the 40% void extruded ZrC is included (Fig. 4) to illustrate this point. It is likely that the postulated void structure gives a smaller radiation heat transfer component than actually noted in the experiments.

D. Factors Which Influence the Thermal Conductivity

Section II reports the effect of vacancies in lowering the thermal-conductivity. The introduction of the porosity, as in the 40% porous ZrC, was also a large step forward in decreasing the heat-conducting power of the

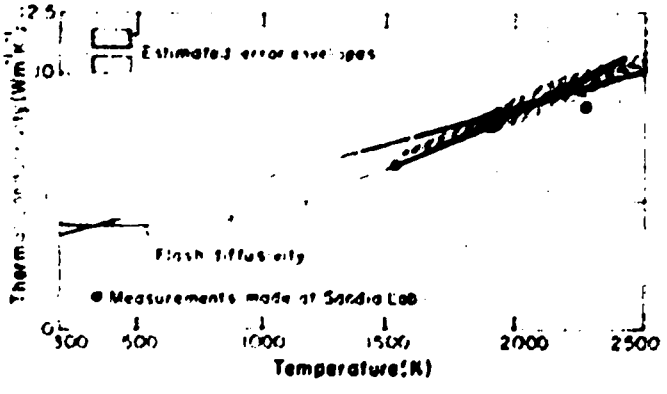

Fig. 2.
Thermal conductivities of 40% porous ZrC shown as a function of temperature.

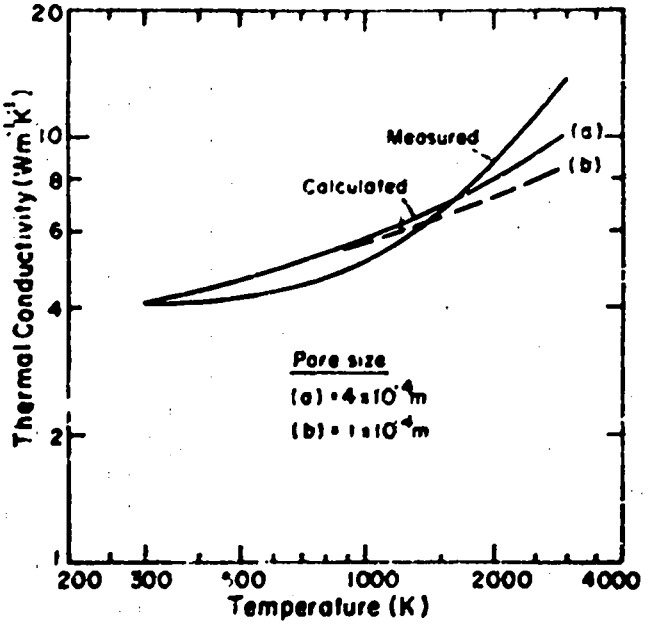

Fig. 3.
Thermal conductivities vs temperature for 40% porous ZrC. Comparison of experiment with values calculated for two porosities.

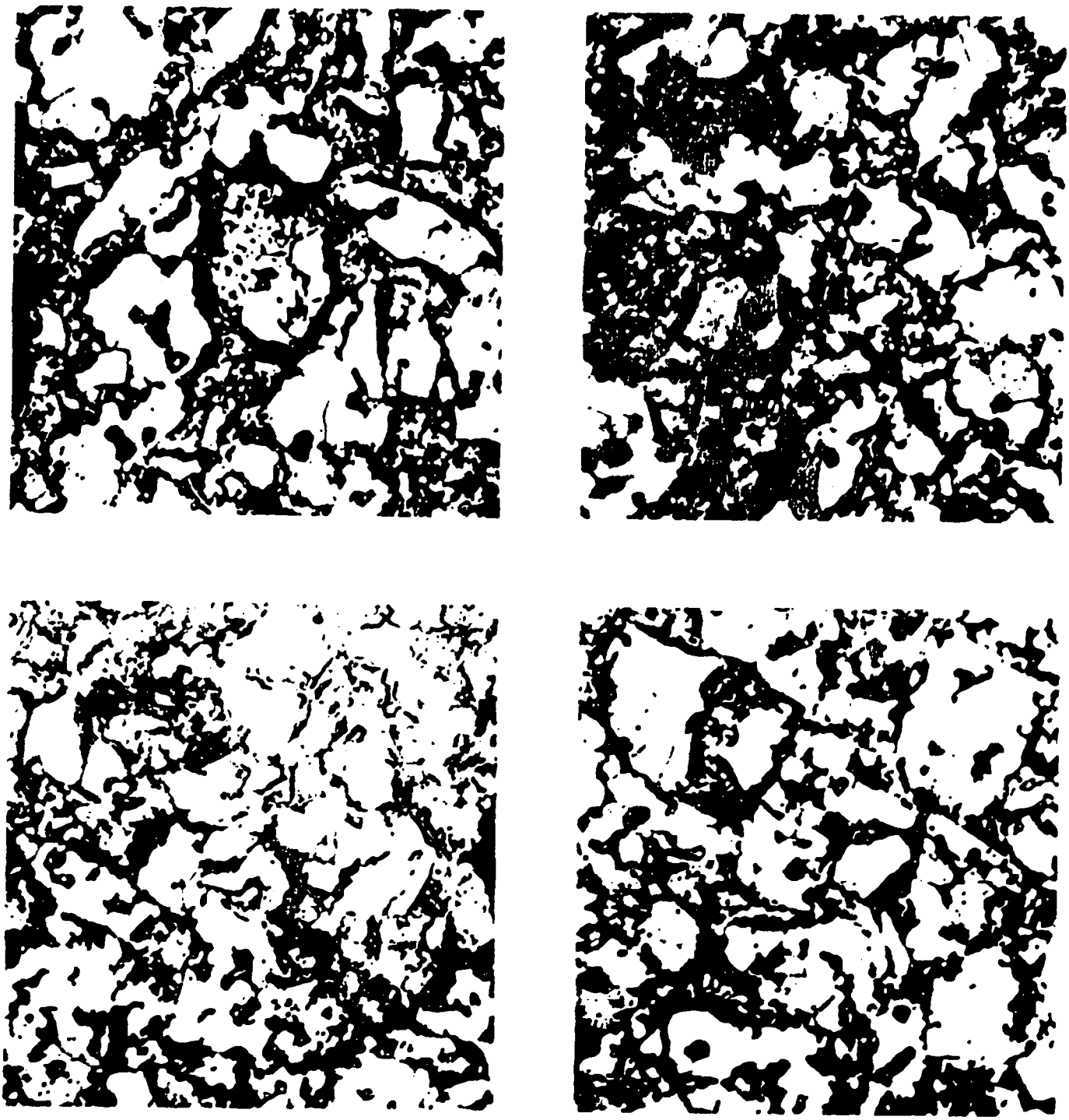

Fig. 4.
Photomicrograph of 60% dense extruded ZrC (150X).

insulator. These two factors operate in parallel; therefore, the insulator system may be generalized by the following formula (Matthiesen's Rule).

$$R_{Total} = R_{Matrix} + R_{Pores} + R_{Interfaces}$$

Here, R is the thermal resistance and is equal to λ^{-1}. Factors that influence λ fall into one of the categories on the RHS of the equation, and will be discussed separately.

R_{Matrix}: The effect of vacancies has already been discussed. It has been demonstrated that optimizing the C/Zr ratio can decrease λ by 3 to 4 times[17] even in the

40% void ZrC. Chafik[18] reported that when the C/Zr ratio is greater than one, that is, when the phase limit is exceeded and the ZrC contains excess carbon, λ may increase sharply. This conclusion is neither confirmed nor denied in the work done at LASL. It has been confirmed that the introduction of nitrogen or oxygen at elevated temperatures will elevate the thermal conductivity.[19] In this case, the oxygen or nitrogen atoms occupy vacancy sites in the carbon sublattice; the effect in elevating λ is not as large as if the sites were occupied by carbon atoms, but it is considerable. For example, $ZrC_{0.96}$ (40% porous) when exposed to nitrogen at 1773 K for 23.4 ks (6-1/2 h) underwent an unambiguous increase in λ of a factor of 2 or greater.[19]

R_{Pores}: Introducing porosity will increase the thermal resistance of a system unless the λ contribution from radiation or from contained gases is intrinsically greater than that of the matrix. To some degree this is attributable to the increase in the tortuosity of the heat-flow path. The shape of the pores, as well as their concentration, influences the increase in tortuosity. For example, pores shaped like platelets with their largest dimensions normal to the direction of the flow of heat would cause a greater impedance than would pores oriented so that the long dimension was parallel to the heat-flow path. For this reason, it is not possible to correlate properties such as the thermal conductivity with the densities of the manufactured ZrC without completely characterizing the concentration, structure, and distribution of the included voids. Figure 4 emphasizes the difficulty in doing this. Similar complications arise when analyzing the influences of gaseous conduction in the pores and when considering radiation heat transport.

$R_{Interfaces}$: The degree of intimacy of contact will define the ability of the interface to carry the heat. It has been demonstrated that the thermal transport mechanism is by phonons and electrons and any disruption of the periodicity of the lattice (grain boundaries, crystallite interfaces, etc.) will increase the thermal impedance. Large particles would have relatively large masses of matrix and few intercrystalline junctions and would be expected to demonstrate relatively high thermal impedances. Mixing particles with a wide range of sizes would increase the number of interconnections between particles with a relatively small increase in total mass, thus decreasing the net thermal resistance. These effects have been observed in the 40% porous ZrC. This point is made in Sec. IV.C: by varying the relationship between the continuous matrix and the fixed bed, the thermal conductivity may be varied.

E. Properties of the Production Porous ZrC

Room-temperature thermal conductivities were measured on samples taken from a large production run. The sample materials were nominally 38% porous, extruded, leached ZrC microslates collectively labeled Lot 4887. The material was single phase, with no free carbon, and with a C/Zr = 0.96 (i.e., $ZrC_{0.96}$). Measurements of λ(300 K) were done on 88 samples.[20] The results are displayed in Fig. 5 where the measured thermal conductivities are plotted against the frequency of the appearance of λ, tabulated in 0.1 W m^{-1} K^{-1} units. The average λ for all 88 samples is 6.8 W m^{-1} K^{-1} with a standard deviation (σ) of 1 W m^{-1} K^{-1}. Eighty-four of the 88 determinations fall within the 95% limit (± 2σ). Densities averaged 4.10 Mg m^{-3} (4.10 g cm^{-3}) with a standard deviation of 0.13 Mg m^{-3}. Three of the above specimens were subjected to hydrogen at 2575 K, at a pressure of 3.1 MPa (450 psi) for 3.6 ks in an effort to leach out some of the carbon.[17] At the conclusion of the experiment the C/Zr had decreased from 0.96 to 0.86 and the average of the λ(300 K) was 3.4 W m^{-1} K^{-1}.

Measurements made on the linear thermal expansion of the 40% porous extruded ZrC yielded results identical to those listed in Sec. II of this report. As expected, the porosity had no significant effect on the CTE. Little additional work was done in this area because engineering information could be taken from the measurements made on the dense material.

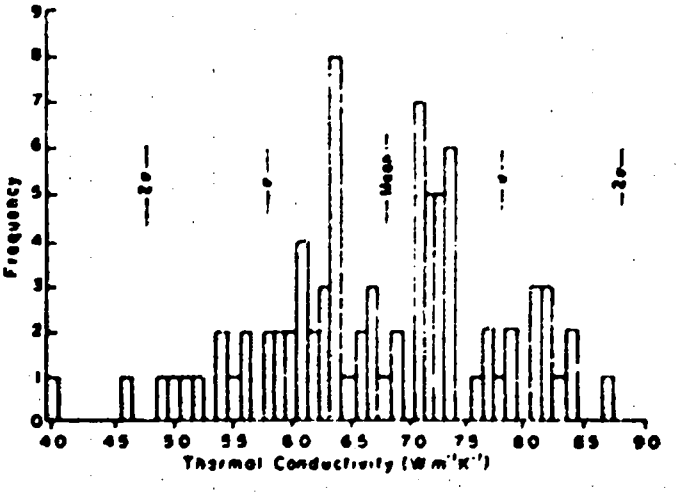

Fig. 5.
Frequency distribution for thermal-conductivity measurements of porous ZrC insulators from NF-2 production run (Lot 4887 Zr).

Because of the minimal strength requirements placed upon the insulators used in the reactors associated with the Rover program, little effort was expended in this area. Some exploratory work was done[21] on the compressive strength properties of the extruded ZrC and the results are shown in Table III.

During the course of the high-temperature, steady-state, thermal-conductivity measurements,[5] surprisingly high-temperature gradients were attained, and survived, by the test specimen. For a long hollow cylinder, resistance heated and cooled by radiation on its outer surface, the maximum tensile strains occur on the outer surface and are given by

$$\epsilon_\theta = \epsilon_z = \alpha \left[\bar{T} - T_{min}\right] \quad .$$

where ϵ_θ and ϵ_z are the maximum tensile strains in the azimuthal and axial directions, α is the instantaneous coefficient of thermal expansion at temperature $\bar{T}$, $\bar{T}$ is the mean temperature of the cylinder, and T_{min} is the minimum temperature which occurs at the outer wall.

If the thermal conductivity and the power density are constant across the wall of the specimen, then the quantity $(\bar{T} - T_{min})$ can be related to the measured quantity $T_{max} - T_{min}$ by the following equation.

$$\frac{\bar{T} - T_{min}}{T_{max} - T_{min}} = \frac{\frac{1}{2} - \frac{3}{2}a - \frac{a \ln a}{\frac{1}{a} - 1}}{1 - a + a \ln a} \quad .$$

where a is the square of the ratio of outer radius to inner radius.

The ZrC extrusion used survived temperature gradients as high as 150 K at the higher temperatures, which corresponds to a strain of 0.1% that was survived by the specimen. This is surprisingly high for a brittle material such as ZrC and suggests that creep and/or plastic flow can relieve thermal stresses in this material at high temperatures.

TABLE III

SOME COMPRESSIVE DEFORMATION AND STRENGTH PROPERTIES OF POROUS, EXTRUDED ZrC

Sample porosity (%)	Temperature (K)	Stress (MPa)	Deformation Rate $(ks)^{-1}$
40[a]	1673	7.0	0
40[a]	2775	0.7	0.003
40[a]	2775	2.1	0.0167
40[a]	2775	7.0	0.0556
34[b]	1673	7.0	0
34[b]	2775	0.7	0
34[b]	2775	2.1	0.0028
34[b]	2775	7.0	0.0194

[a] Oriented parallel to the extrusion axis. Ultimate strength at 300 K, 123 MPa.

[b] Oriented perpendicular to the extrusion axis. Ultimate strength at 300 K, 186 MPa.

F. Reactor Performance of the Porous Extruded ZrC

Two of the 49 cells in LASL's Nuclear Furnace No. 1 used ZrC in the interstices between the fuel element and the water-cooled cell wall (the other cells used pyrolytic graphite). The function of the ZrC was that of a barrier and a spacer for keeping the fuel element centered. The hydrogen that flowed in the channel provided the necessary insulation. The configuration of the NF-1 ZrC is shown in Fig. 6. These tests are the only in-reactor tests made using ZrC, and they provide some qualitative information on the ability of the ZrC to withstand the environmental combination of hydrogen at 2700 K temperatures and the radiation field. The postmortem work on NF-1 was not completed when the Rover program was cancelled. The ZrC spacers showed longitudinal cracks; however, because of the tight dimensions, it was not clear whether the cracks were formed by mechanical loading during the reactor heat-up or by thermal stress. The general appearance of the ZrC weighted the

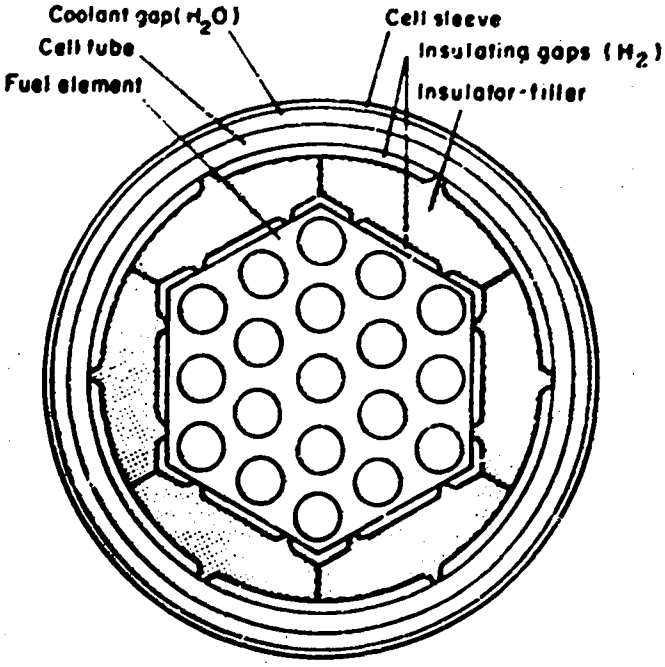

Fig. 6.
Cross section of NF-1 cell showing location and shape of the experimental porous ZrC insulators.

mechanical loading rationale. There were no indications of reaction with hydrogen nor any indication of any form of degradation in the appearance of the material. The one thermal-conductivity measurement was made on a sample taken from a section halfway between the cold inlet and the hot-gas exit which should have seen the maximum temperature and radiation field intensity. The thermal conductivity of this irradiated ZrC was 3.2 $W m^{-1} K^{-1}$ at 300 K, which may be compared with the NF-1 production λ(300 K) of about 4.5-5.0 $W m^{-1} K^{-1}$ (Lot 4706) listed in Table II. The expected change in λ from the introduction of a high concentration of point defect scattering centers is not an unreasonable value.

V. VERY POROUS ZrC MADE FROM CARBON FIBERS

The insulator system chosen for NF-2 and the system that would have been used for high-performance flight reactors was made by the solid-gas reaction of carbon fibers with $ZrCl_4$. Because of the compressed time scale (the decision to use ZrC made in this manner was made about seven months before the "parts on hand" date) the development, evaluation, and production proceeded along parallel paths. As a result, descriptions of production and properties of the very low-density ZrC are inevitably tied to the NF-2 design needs. A discussion of the porous, fiber-based ZrC would include an interlacing of various aspects of these factors. Appendix C is a LASL internal document describing some aspects of the fabrication of the NF-2 insulator units.

Figure 7 is a sketch of the NF-2 insulator configuration. The reactor consisted of 49 such cells. We expected that the fuel element would run as hot as 2900 K; the aluminum tube was water cooled and the inner surface of the aluminum tube was not expected to exceed 500 K. Thus, the 2400 K temperature drop would have to be taken by the ZrC insulator; and since the mean thickness was about 4.0 mm (5/33 in.), the extent of the insulating power required is amply demonstrated (Fig. 8). Figure 8 shows the radial heat-flow leak vs the value of λ for the insulator configuration shown in Fig. 7 and for the full-power operation for an NF-2 cell. Figure 8 shows that to transfer 95% of the thermal energy to the coolant gas, a 300 K λ of about 0.5 $W m^{-1} K^{-1}$ would be required. This then set the goal for the NF-2 insulator design and for the target thermal conductivity of less than 1 $W m^{-1} K^{-1}$ at 300 K.

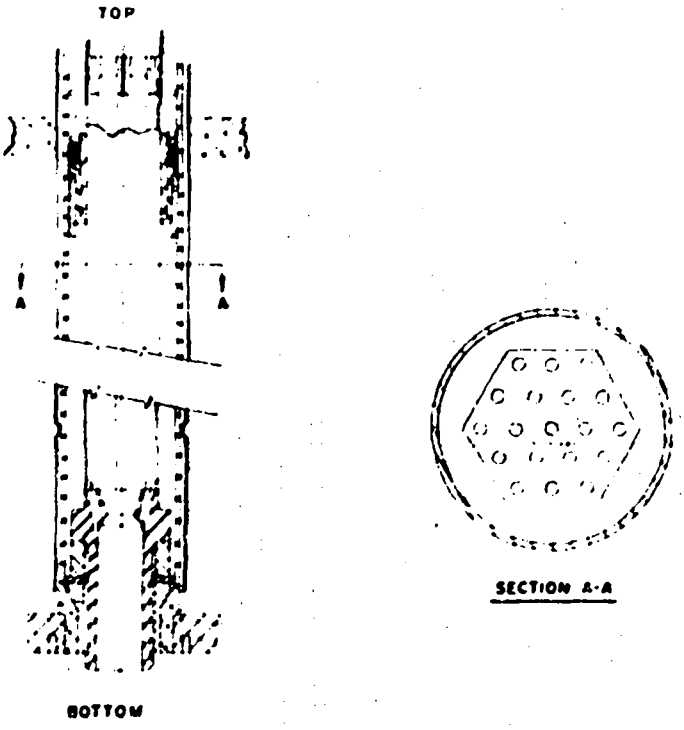

NF-2 INSULATOR

Fig. 7.
NF-2 ZrC insulator configuration.

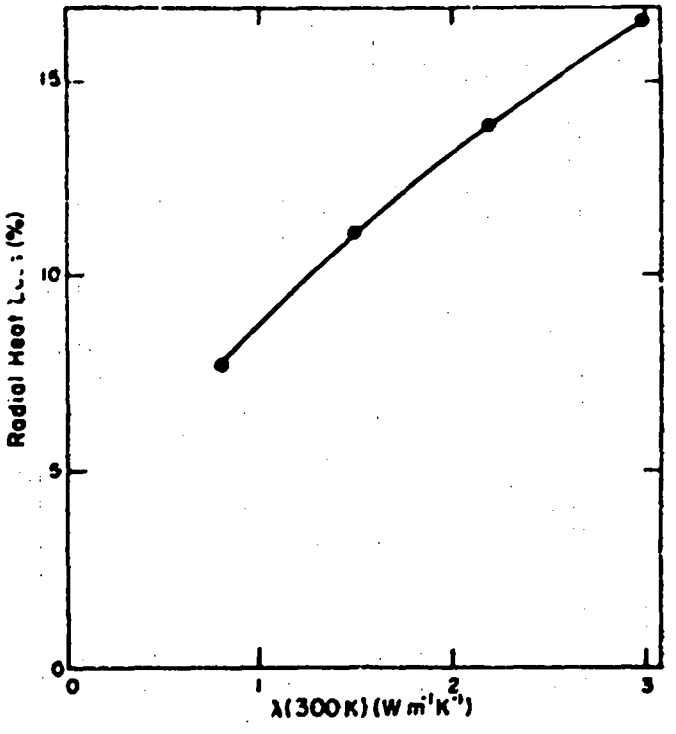

Fig. 8.
Relation between radial heat leak and λ (300 K) for NF-2 insulators.

A. Fabrication

The NF-2 insulator units were produced in a multiple-step, single-pass operation. The tubular carbon-fiber raw material was premachined to approximate cross-section dimensions and was converted directly to the final product. The starting material and the finished product are shown in Fig. 9. The carbon-fiber tube was converted to ZrC by exposure to a mixture of $ZrCl_4$,H_2, argon, and HCl at 1600 K for 40 h, which resulted in a product composition of $ZrC_{0.95}$ and a 76% porosity (24% theoretical density). The temperature was then dropped to 1500 K and CH_4 was added to the gas mixture; under these conditions, a coating of ZrC was deposited on each fiber. After 10 h of this latter treatment, the porosity was decreased to about 72%. Finally, the temperature was raised to 2800 K and the insulators were held at this temperature in an argon environment for 2 h. The insulators were ready for final machining after they were removed from the conversion furnaces. Figures 10, 11, and 12 are scanning electron micrographs of the carbon fibers, the converted ZrC, and the fiber-coated converted ZrC, respectively. Note that the fiber coating increases the degree of filleting and fiber interconnection. Intuitively it would be expected that fiber coating would increase both the strength and the thermal conductivity, which proved to be the case. The 2800 K heat treatment seemed to counteract the coating effects by decreasing the thermal conductivity, although the reason for this phenomenon is obscure.

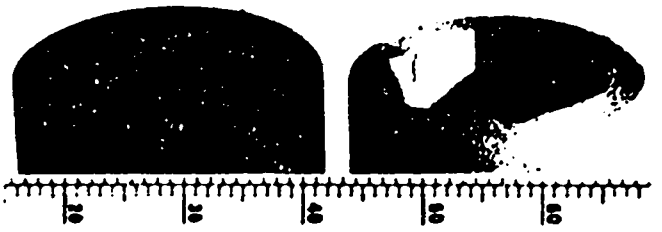

Fig. 9.
The carbon-fiber tube before conversion and the finished ZrC product (right).

Fig. 10.
Scanning electron micrograph of carbon-fiber starting material (1000X).

Fig. 11.
Scanning electron micrograph of fiber ZrC after conversion (1000X).

Fig. 12.
Scanning electron micrograph of ZrC after conversion and vapor-deposited ZrC fiber coat (1000X).

B. Thermal Conductivity of Very Porous ZrC at 300 K

All the thermal-conductivity measurements made at 300 K on the very porous ZrC were made with the flash-diffusivity method. Despite all the precautions taken to assure the accuracy of such measurements (see Sec. IV.A), unpublished work done in LASL Group N-7, just before the group was dissolved, indicated that the flash-diffusivity measurements yielded answers that were too high. The insulating power of the ZrC insulators, as reported in this document, is probably pessimistic and the fibrous ZrC insulators are, in fact, more effective than the numbers indicate. Results of λ measurements made at 300 K using the flash-diffusivity method[22,23] are compiled in Table IV. This work was done independently by two investigators with essentially identical results and shows the variation of thermal conductivity with degree of completeness of the fabrication. The increase in λ due to the fiber coating is explained by the increase in the intimacy of contact of the fibers and by a slight increase

TABLE IV

ROOM TEMPERATURE THERMAL CONDUCTIVITY OF PRODUCTION POROUS FIBER-ZrC

Sample Condition	Porosity (%)	λ (300 k)[a] ($W m^{-1} k^{-1}$)	Standard Deviation ($W m^{-1} k^{-1}$)
Converted to ZrC	74	0.65	
	71	0.65	
	75	0.62	
	73	0.85	
	79	0.42	0.04
	75	0.45	0.04
Fiber coated	66	1.00	0.10
with ZrC	65	1.32	0.25
After 2800 k	92	0.35	
heat treatment	72	0.35	
	72	0.43	0.04
	72	0.36	0.02

[a]Measurements made in air.

in the density. Table IV shows that the heat treatment is very effective in reducing λ, but before we could make further studies, the project was terminated.

Figure 9 shows a void orientation in the converted ZrC in the form of circumferential cracks. This was a particularly fortunate development because such cracks serve as thermal-stress fracture relief modes and, because of the configuration of the insulator (Fig. 7), would not be expected to have deleterious effects on the reactor operation. Another consequence of this void structure was the introduction of an anisotropy in the thermal conductivity. Measurements made parallel and perpendicular to the insulator tube axis showed that this anisotropy could be as large as a factor of five.[25] The effect of the cracks as thermal barriers was great enough that having a $C/Zr = 0.95$ proved to be no disadvantage; as a matter of fact, this slightly high value resulted in a product with more desirable handling and machining characteristics than the systems with lower carbon contents.

C. Modeling the Very Porous ZrC Insulators

Before discussing the high-temperature measurements of the very porous ZrC, it is necessary to consider the mechanism by which heat is transferred in a heterogeneous medium of this type. In principle, the modeling

rationale is the same as that discussed in Sec. IV.C for the 40% void ZrC. In practice, the situation is far more complex.[26] In the very porous systems, with porosities in the 70 to 95% region, the nature of the voids will be important in determining the thermal conductivity, not only at temperatures where the radiation is effective but also at lower temperatures where the nature of the gas in the voids is significant. The critical factor is the description of the pores; however, Figs. 10, 11, and 12 show that characterization of such a void structure presents a formidable problem. Added to this are the anisotropic effects described in the previous section. Thus, altering the ratio of the continuous-fiber ZrC to the fixed-bed ZrC and changing the void structure afford an endless group of combinations. This is the heart of the ZrC system. For a given density, the variations described permit the fabricator to tailor the value of the thermal conductivity and related properties (Fig. 13). In Fig. 13 we assumed that the fiber diameter was fixed, that a pore diameter could be assigned to the system, and the overall porosity of the ZrC was taken to be 80%. The three curves were generated by varying the ratio of the fixed bed to the continuous ZrC, by including the effect of the hydrogen at 3.4 MPa (500 psi), and by thermal radiation effects. The hydrogen effects were included originally because there are no facilities available for measuring λ in high-pressure hydrogen at elevated temperatures. Hydrogen effects were included here to illustrate the drastic effects that the environment may have on the intrinsic properties of such a porous material (compare Figs. 13 and 2).

Practical lower limits of the thermal conductivities to be expected from highly porous ZrC were calculated and the results are displayed in Fig. 14. Here the pore structure was taken to be similar, except for the magnitude of the void fraction; the matrix structure was fixed (i.e., ratio of the continuous ZrC to the fixed bed = constant). Thermal-conductivity measurements were calculated for the insulators with radiation, and hydrogen gas inclusion at 3.4 MPa was considered. Porosity effects are of a magnitude similar to that effected by changing the matrix structure (Fig. 13). This was important in fabrication considerations because it demonstrated clearly that the ZrC could be fabricated with densities high enough to retain any required structural integrity without sacrificing the desirable insulating properties.

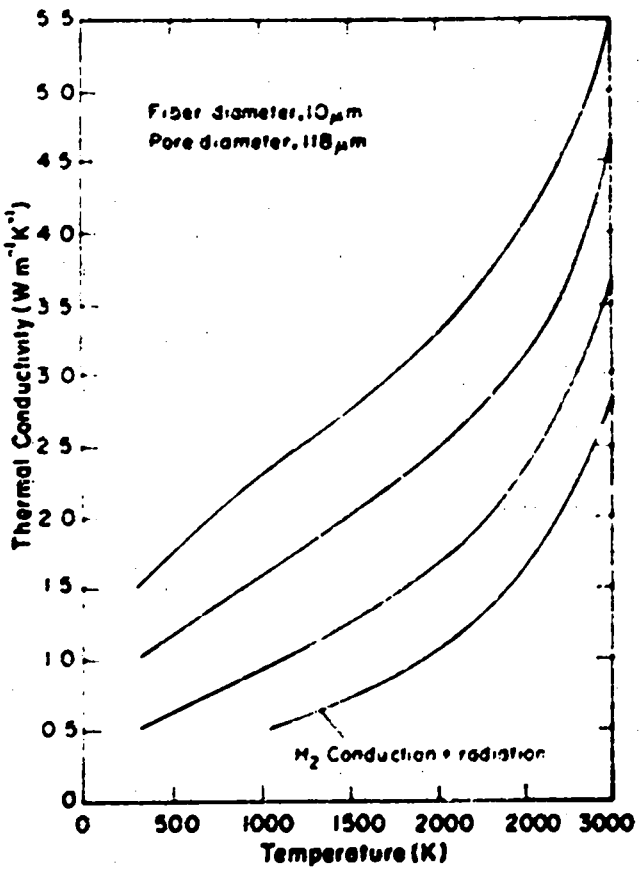

Fig. 13.
Calculated thermal conductivities for 80% porous ZrC.

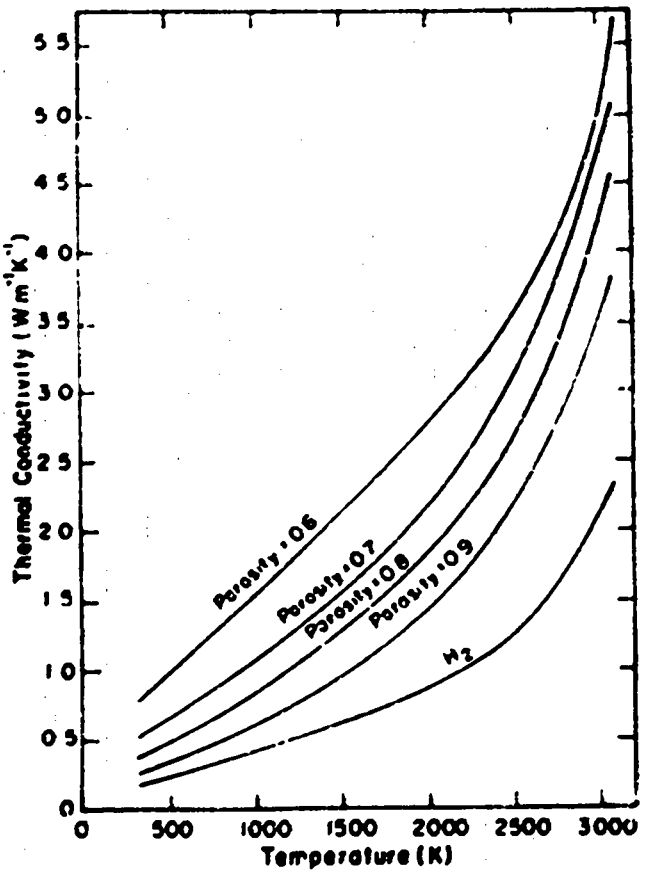

Fig. 14.
Calculated limiting values for thermal conductivities of ZrC of different porosities.

These ideas were tested by making thermal-conductivity measurements of very porous ZrC at elevated temperatures. A ZrC tube (with 84% porosity, C/Zr = 0.93, and fabricated expressly for this purpose) was used for steady-state radial heat-flow measurements of λ(T) in vacuum from 1300 to 2450 K.[27] These data are shown in Fig. 15 where the experimental points, fitted curve, and predicted[16,26] curve are compared. As shown in Fig. 2, the upturn of the experimental data at the high temperatures is somewhat greater than would have been predicted; however, the difficulty in characterizing the void structure is probably at the root of this problem and was not solved when efforts in this area ceased.

D. High-Temperature Thermal Conductivity of NF-2 Insulators

Samples cut from production NF-2 insulators were used for thermal-conductivity measurements using the laser-flash technique λ[α(T)] from 300 to 2200 K.[24] These measurements were made in vacuum. Because of the inherent uncertainties associated with the λ[α(T)] method for these very porous materials, the data are shown along with normalized predicted values of the thermal conductivity[16,26] in Fig. 16. The material used had a porosity of 72%, was heat treated, and had a λ(300 K) in air of 0.38 W m^{-1} K^{-1}. As in other comparisons of this type, the agreement is quite good until temperatures in excess of 2000 K are reached, then the experimental data rise faster with temperature than would be expected.

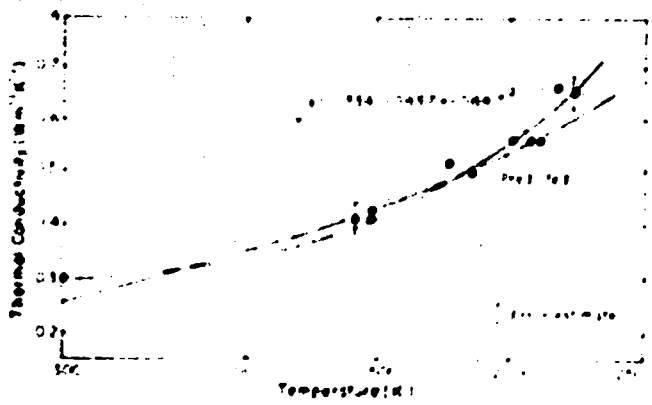

Fig. 15.
Comparison of predicted thermal conductivity with experiment for 84% porous fiber ZrC.

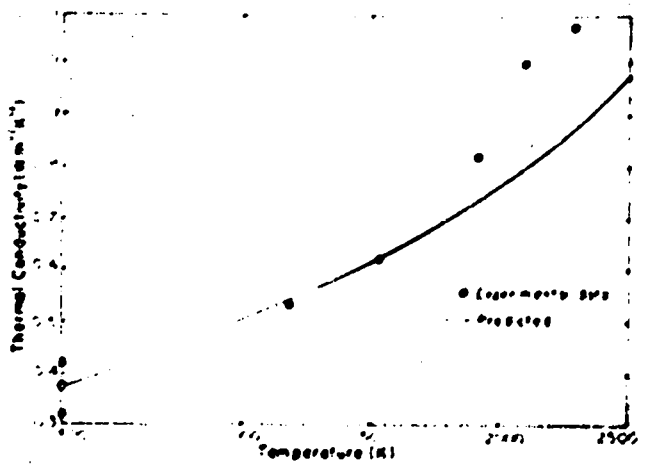

Fig. 16.
Thermal conductivities of NF-2 production insulators compared with predicted temperature trend.

E. Effect of Temperature on the Compressive Strength of ZrC

It was necessary to define the temperature limits of the usefulness of the insulators in terms of their resistance to compressive stress.[28] Standard NF-2 production materials (72.5% porosity, $ZrC_{0.96}$, heat treated at 2800 K) were subjected to compressive stress from 300 to 3073 K. The stress was applied parallel to the cylinder axis of the insulator units with a fixed strain rate of 42.3 μmsec^{-1}. These tests were done at 300, 1273, 1873, 3073, 2273, 2473, 2773, and 3073 K, in a helium environment. The strength of the ZrC was (somewhat arbitrarily) defined as that stress level where yield first occurred. From the data generated during these experiments, it appeared that the yield time was short enough to make the creep phenomena unimportant. The curve showing the effect of temperature on the yield stress for these materials is given in Fig. 17. The shape of the curve is reasonably characteristic of that for a brittle material which undergoes plastic deformation at temperatures greater than half the melting temperature. The data suggest that 3100 K is an upper limit for ZrC use to avoid excessive deformations.

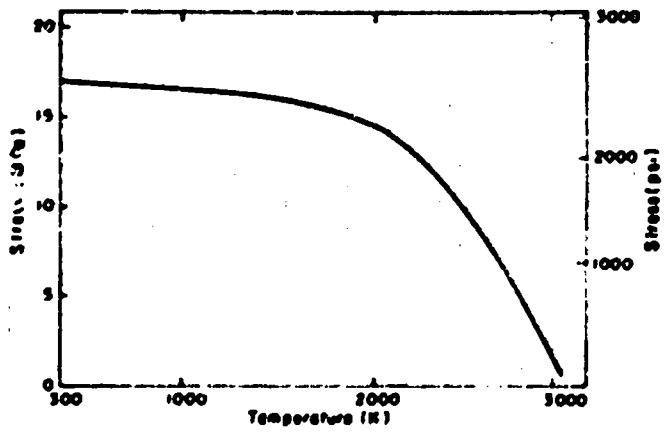

Fig. 17.
Effect of temperature on yield stress for 72.5% porous fiber ZrC.

F. Insulator Simulation Tests

The porous fiber-based ZrC was never reactor tested. NF-2 was scheduled for testing when the Rover program was cancelled. As part of the performance evaluation of the insulator units, a test was made to investigate the behavior of ZrC in a simulated NF-2 fuel cell.[29] An 8-cm-long piece of full cross-section NF-2 insulator was slipped over a standard thermal-stress fuel element specimen (Fig. 7). The insulator was centrally located on the fuel element so that the heat flux was normal to the insulator axis. The outer surface was free to radiate to the water-cooled furnace wall. This insulator came from an early NF-2 production run. It was converted but was not fiber-coated and had not been heat treated. The insulator was 77% porous (23% theoretical density). The test procedure was the same as that followed for a fuel element thermal-stress fracture experiment where the coolant flow is established and the power is increased until the specimen fractures. In this case, the test was terminated by the fracture of the fuel element at a power density of about 4050 MW m^{-3}. At the conclusion of the test, the insulator was cracked but did not break up. The minimum temperature drop across the insulator unit was estimated to be 1000 K. Based on these very rudimentary experiments, (the only simulation experiments performed) the outlook for a satisfactory reactor performance from the porous ZrC insulators was optimistic.

Similar evaluation tests[30] were made on converted and fiber-coated ZrC tubes (63% porous). These insulators were made expressly for evaluation purposes. These tubes were subjected to temperature gradients as great as 900 K across the tube walls. Examination of the insulators after two cycles revealed no significant changes in the structure. These tests suggest that the fiber-coating process improved the structural integrity of the fiber ZrC under high-temperature test conditions.

G. Production Evaluation and Quality Assurance

The only figure of merit available for the entire production run of about 500 insulator units was the gross density. Some nondestructive measurements of density variations along the length of the insulator units were also made. From these two sets of information, two facts appear: the density was not uniform within the insulators, and the gross density of the insulator units was dependent on the position it had occupied in the conversion furnace. If the densities are broken down according to furnace positions, there are four groups of about 125 insulators each and, with this size sample, a meaningful standard deviation was calculated (Table V). So far as could be determined during the insulator evaluation work, these variations in densities, in the individual insulator units and for the insulator production as a whole, were insignificant. The variation seen in measured properties had an undetectable effect on the anticipated (in the reactor) and measured performances.

TABLE V

GROSS DENSITIES OF ZrC INSULATOR PRODUCTION

Furnace Position	Gross Density % theoretical	Standard Deviation (%)
Top	30.09	4.0
Middle upper	28.48	4.0
Middle lower	28.01	3.5
Bottom	28.04	2.0

Techniques for making measurements $\{\lambda(\alpha)\}$ of the overall average thermal conductivity for an entire insulator unit at room temperature had been developed. The plans called for a 100% survey of the production insulators to pass on to the reactor operation personnel the best values for λ. Unfortunately, the $\lambda(\alpha)$ techniques developed had just proved effective for this task when the efforts ceased. The only number reported for an insulator unit was 0.8 W m^{-1} K^{-1} at 300 K. Little more than this was reported. It did appear, however, that the goal for fabricating a pure ZrC insulator with a thermal conductivity of less than 1 W m^{-1} K^{-1} had been reached.

H. Insulators and Reactor Design

A very brief outline of the design concepts for which the insulator applications were intended is given in Appendix D. The likelihood that the porous ZrC insulators could be tailored to fit the designs then on the drawing boards, or being evolved, was very good.

VI. SUMMARY

The development of a satisfactory substitute for the pyrographite insulators, which had been used in all but the very last of the Rover reactors, was very successful. The overall loss of insulating power due to the change to the substoichiometric porous ZrC occurred largely at elevated temperatures and was of a manageable magnitude. After considering other properties, including density, strength, thermal-stress resistance, chemical

inertness, ease of procurement, controllability in fabrication, uniformity of production, and machinability, we favored the ZrC as the more desirable insulator system. The details in this report demonstrate the flexibility of the ZrC and related carbides and indicate, in a very positive manner, the desirability for using the carbides, in particular ZrC, where such flexibility in physical properties might be required.

VII. ACKNOWLEDGMENTS

The coordination of the ZrC development program was accomplished by an interdivisional group known as the "Insulator Committee." When the Rover program terminated, the Committee consisted of the following personnel.

Paul Wagner, N-7 (Engineering Analysis Group), Chairman
Allen R. Driesner, N-1 (Materials Group)
Edmund K. Storms, CMB-3 (High-Temperature Chemistry Group)
James M. Dickinson, CMB-6 (Fabrication Group)
Thomas J. Merson, N-3 (Engineering Design Group)
Herbert J. Newman, N-3 (Engineering Design Group)

The work reported here could not have been accomplished without the unstinting efforts of each Committee member. Without the support of J. C. Rowley, R. W. Spence, M. G. Bowman, T. C. Wallace, and others from CMB, M, N Divisions, and 5D-1 this work would not have been possible.

Special acknowledgment is given to Filmore F. Criss whose imaginative efforts in the development of the fiber ZrC insulator were invaluable.

REFERENCES

1. V. S. Neshpor, S. S. Ordan'yan, A. I. Avgustinik, and M. B. Khusidman, "The Effect of the Chemical Composition of Zirconium and Niobium Carbides in the Homogeneity Region on Their Electric and Thermal Properties," National Aeronautics and Space Administration report NASA-TT-F 9350 (April 1965).

2. P. G. Klemens, "Thermal Resistance Due to Point Defects at High Temperatures," Phys. Rev. 119, 507-509 (1960).

3. R. E. Taylor, "Thermal Conductivity of Zirconium Carbide at High Temperatures," J. Amer. Ceram Soc. 45, 353-354 (1962).

4. L. N. Grossman, "High Temperature Thermophysical Properties of Zirconium Carbide," J. Amer. Ceram. Soc. 48, 236-242 (1965).

5. P. Wagner and H. D. Murphy, "Steady-State Thermal Conductivities for Extruded Porous ZrC at High Temperatures," Los Alamos Scientific Laboratory (Group N-7) internal document (February 18, 1972).

6a. G. V. Samsonov and V. Ya. Naumenko, "Thermal Expansion of the Carbides of the Transition Metals of Group IV-V in Their Homogeneity Range," Teplofizika Vysokikh Temperatur 8, 1093-1095 (1970).

6b. V. G. Bukatov, G. A. Rymashevskii, and V. B. Fedorov, "Thermal Expansion of Nonstoichiometric Zirconium Carbides," Izv. Akad. Nauk. SSSR, Neorg. Mater. 7, 519-520 (1971).

7. J. O. Gibson, "Low Thermal Conductivity ZrC-Graphite Fiber Reinforced Composite Studies," McDonnell Douglas Astronautics Laboratory report MDC G 3125 (July 1971).

8. P. Wagner, "ZrC Made from Converted Krebs Foam (Box 100)," Los Alamos Scientific Laboratory (Group N-7) internal document (October 11, 1972).

9a. P. Wagner and L. B. Davelsberg, "Thermal Conductivity of ZTA Graphite," Carbon 5, 271-279 (1967).

9b. W. L. Sibbitt, "Discussion of Conductivity Values as Obtained from the Comparison Probe Technique and Those Computed from Diffusivity Values," Los Alamos Scientific Laboratory (Group N-7) internal document (April 16, 1971).

9c. W. L. Sibbitt, "Thermal Conductivity of a Test Sample of Iron," ibid. (April 9, 1971).

9d. H. D. Murphy, "Room Temperature Flash Diffusivity of a Fired, Grade A Lava Tube," ibid. (August 10, 1971).

9e. P. Wagner, "Thermal Diffusivity Measurements on Grade A Lava and on Code 9606 Pyroceram," ibid. (August 11, 1971).

10a. P. Wagner, "Thermal Diffusivity and Conductivity of Porous ZrC, Extrusion Lot No. 4706-2," ibid. (August 23, 1971).

10b. W. L. Sibbitt, "Thermal Conductivity of Extruded ZrC Ribbon Insulators (4706 Series)," ibid. (September 7, 1971).

10c. B. H. Morrison, "Room Temperature Thermal Diffusivity and Conductivity of Porous ZrC Extrusion Lot No. 4706-2," ibid. (September 9, 1971).

10d. P. Wagner, W. L. Sibbitt, and B. H. Morrison, "Thermal Conductivity of Porous ZrC at Room Temperature: Review and Summary," ibid. (January 28, 1972).

11. P. Wagner, "Thermal Conductivity of Porous ZrC Using an Axial Flow, Steady-State Comparison Apparatus," ibid. (January 25, 1972).

12. P. Wagner, "Colora Measurements on ZrC Lot 4706," ibid. (November 19, 1971).

13. B. H. Morrison, "Thermal Diffusivity-Conductivity of Porous, Extruded ZrC (Lots Nos. 4558 and 4575) from 300 K to 2600 K," ibid. (February 11, 1972).

14. P. Wagner, "Comparison of High Temperature Thermal Diffusivities of Porous ZrC. Results on Lot 4706 Measured at LASL and Sandia Laboratories," ibid. (December 22, 1971).

15. W. L. Sibbitt, "Thermal Conductivity of Extruded ZrC Ribbon Insulators (4705 Series)," ibid. (October 10, 1971).

16. W. L. Sibbitt, "A Model of the Porous Insulators," ibid. (January 24, 1972)

17. P. Wagner, "Effect of High Pressure Leaching on Porous ZrC Lot No. 4887," ibid. (July 26, 1972).

18. E. M. Chafik, "Ein Verfahren Zur Messung der Temperaturleitzahl fester Stoffe bei hohen Temperaturen unter Anwendung eines modulierten Lichtstrahls," PhD thesis, University of Stuttgart (W. Germany), (April 1970)

19a. P. Wagner, "Thermal Conductivity of Porous ZrC: Effect of Exposure to N_2 at High Temperatures" (in two parts), Los Alamos Scientific Laboratory (Group N-7) internal document (January 11 and 25, 1972).

19b. P. Wagner and H. D. Murphy, "Stabilization of Porous, Extruded ZrC for High Temperature Experiments," ibid. (April 4, 1972).

20. P. Wagner, "Thermal Conductivities of Lot 4887, Porous ZrC Insulators for NF-2," ibid. (May 4, 1972).

21. A. R. Driesner and R. G. Merryman, "Mechanical Properties of 60% Dense ZrC," Los Alamos Scientific Laboratory (Group N-1) internal document (November 10, 1972).

22. B. H. Morrison, "Room Temperature Thermal Diffusivity-Conductivity of Low Density ZrC for NF-2," Los Alamos Scientific Laboratory (Group N-7) internal document (November 15, 1972).

23. B. H. Morrison, "Thermal Conductivity of Low Density, Fiber Coated ZrC for NF-2 Insulators," ibid. (December 18, 1972)

24. B. H. Morrison and P. Wagner, "Thermal Conductivity of Heat-Treated NF-2 Insulators," ibid. (December 26, 1972).

25. P. Wagner, "Thermal Conductivity (300 K) of Very Porous ZrC," ibid. (September 1, 1972)

26. W. L. Sibbitt, "Predicted Values of Thermal Conductivity of Porous, Fibrous ZrC (A Note Concerning Analytical Methods)," ibid. (July 24, 1972).

27. P. Wagner, "Steady-State Thermal Conductivity of Porous ZrC Tubes at Elevated Temperatures," ibid. (February 21, 1973)

28. P. Wagner, "Effect of Temperature on the Strength of Porous ZrC," ibid. (January 18, 1973).

29. W. R. Prince, "Photograph Showing Performance of NF-2 Porous ZrC Insulator Surrounding a Heated Fuel Element," ibid. (January 5, 1973).

30. W. R. Prince, "Structural and Thermal Performance of Fiber-Coated, Porous, Fibrous ZrC Cylindrical Insulators," ibid. (February 20, 1973).

APPENDIX A

CHARACTERIZATION AND MEASUREMENTS ON ZrC_x

1. EXPERIMENTAL

A. Sample Preparation

The samples were prepared as 12.7-mm-diam by 2.5-mm-thick disks by hot pressing the powdered carbides at 3000 K under a pressure of 100 MN/cm^2 using a graphite die. The billet was ground to the desired diameter and sliced into disks with a wire saw. These disks were then ground to thickness and repurified by heating in vacuum. Measurements were made on three disks from each billet.

B. Sample Characterization

All samples were analyzed for total carbon by combustion in oxygen and for oxygen by platinum fusion. Except when the impurity content was high the remainder of the material was assumed to be the major metal. All samples were single phase and, except for the sample containing sulfur, had sharp powder patterns. Photomicrographs showed a collection of crystals of various sizes and relatively large isolated voids.

C. Thermal-Conductivity Measurements

All measurements of thermal conductivity (λ) were made at 300 K using the flash-diffusivity technique. The description of the apparatus used and its characteristics have appeared in the literature.[1] This equipment is capable of generating data with a standard deviation of about 3% accuracy when used with well-known, well-characterized materials. However, because of the uncertainty in the specific heat and the necessity for correcting all measurements to theoretical density, it is estimated that the accuracy of the reported values of the thermal conductivity will lie within a 5% standard deviation band.

Thermal conductivities were calculated from

$$\lambda = \alpha \rho C_p \qquad \text{(A-1)}$$

where α is the thermal diffusivity, ρ is the density, and C_p is the specific heat. The data were reduced to that for a theoretically dense material by

$$\lambda = \lambda' \frac{2 + P}{2(1 - P)} \qquad \text{(A-2)}$$

Here P is the fractional porosity ($= 1 - \rho'/\rho$) and the primed quantities are the measured values whereas λ and ρ refer to values for the theoretically dense ZrC. In deriving Eq. (A-2), Maxwell[2] assumed that the pores were isolated and isotropic. For the densities of the specimens used in this work, the assumption of pore isolation is reasonable, however, the assumption of pore isotropicity is more difficult to demonstrate and, as such, adds to the uncertainty in the derived results.

D. Density Measurements

The densities used for the calculation of λ from α [Eq. (A-1)] were obtained by measuring and weighing the samples used for the α measurements. Because a knowledge of the theoretical density (ρ) is required for calculating the porosity and because the theoretical density depends on the carbon-to-metal ratio, this also had to be measured. The theoretical densities were calculated from measured lattice parameters for different values of C/M and the dependence of the densities on the C/M ratio was established (Fig. A-1).

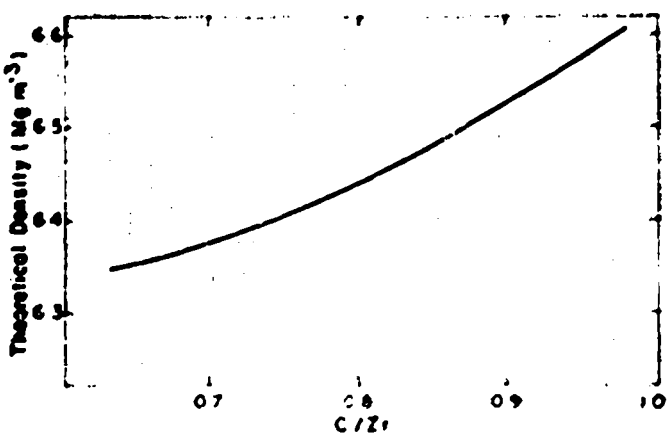

Fig. A-1
Densities of substoichiometric ZrC_x

E. Specific Heat for ZrC_x

The specific heat for NbC_x is known over the C/Nb range considered here. The specific heat for ZrC_x is known only for $ZrC_{0.98}$ (Ref. 3). The Cp's used in Eq (A-1) for ZrC were obtained by estimating these values by analogy with the NbC_x system. This is shown in Fig. A-2 where the NbC and ZrC Cp's are displayed as f(C/M).

F. Electrical Resistivity Measurements

Measurements of electrical resistivity (ρ_R) were made at 300 K using a Kelvin double bridge. The ρ'_R measurements were made on specimens cut from the disk-shaped λ samples, thus the λ' and ρ'_R values were obtained in orthogonal directions. In principle, the direction of measurement should not influence the results because the samples used were polycrystalline and ZrC has a rock-salt structure. The electrical conductivities ($= 1/\rho_R$) were reduced to the value for the theoretically dense material by Eq (A-2).

II. RESULTS

A. ZrC

The data obtained during the experimental investigations on ZrC and NbC are compiled in Tables A-I and A-II. As shown in the tables, not all the data were gathered on all the samples because the samples were prepared for very specific purposes. For example, as seen in Table A-I, some of the samples were purposely prepared with large amounts of impurities so that the relative effects of vacancies and impurities could be compared. The relatively large concentrations of oxygen and sulfur did not affect the electrical and thermal properties nearly so much as did a change in the vacancy concentration (i.e., change in C/Zr). The dependence of the thermal conductivity upon the C/M ratio in the single-phase ZrC and NbC is shown in Fig. A-3. A more detailed curve of λ vs C/Zr is presented in Figs. A-4 and A-5 where the data from this investigation are collected and compared with data taken from the literature [4-6]. Figure A-6 displays the behavior of the electrical resistivity with C/Zr plotted along with ρ_R data and an interpretation of the electrical data in terms of the thermal conductivity. The electronic component of the thermal conductivity was obtained from the Weidemann-Franz relationship

$$\lambda_{el} = \frac{L\,T}{\rho_R} \qquad \text{(A-3)}$$

where the value of L used was that for fully degenerate electronic energy states, $L = 2.45 \times 10^{-8} (v/K)^2$. It appears that on this basis, the electronic component of the thermal conductivity is about 37% from $ZrC_{0.85}$ to $ZrC_{0.95}$. From $ZrC_{0.95}$ to ZrC, λ_{el} may be smaller, however, because of the steepness of the λ and ρ_R curves with C/Zr, measurements of greater accuracy in the dependent and independent variables would have to be made to establish this firmly. With this in mind, it is proposed that for the monophase ZrC system at 300 K,

$$\lambda_{el}/\lambda = 0.37 \text{ and } \lambda_{ph}/\lambda = 0.63 \qquad \text{(A-4)}$$

where λ_{ph} is the phonon contribution to the thermal conductivity.

B. NbC

Four substoichiometric samples of NbC_x were used for λ' measurements. The data obtained on these specimens are shown in Table A-II. The behavior of the thermal conductivity for NbC_x is demonstrated in Fig. A-3 where a striking similarity between the behavior of the λ's for NbC and ZrC can be seen. Further, the electronic component of the thermal conductivity for NbC is of the same magnitude (~34%) as that calculated for ZrC.

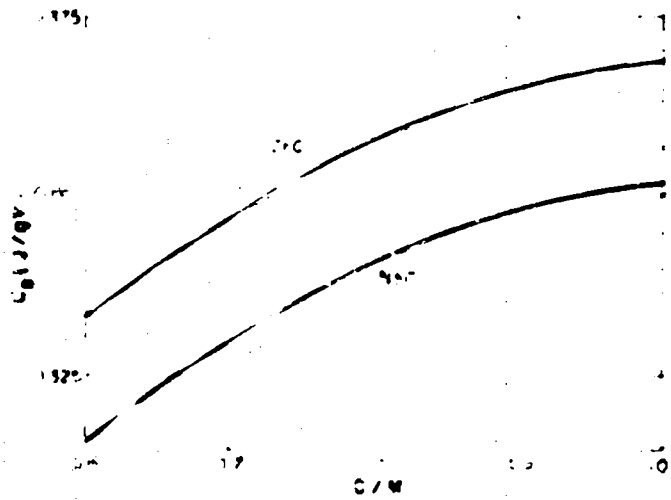

Fig. A-2
Heat capacities of substoichiometric NbC_x and ZrC_x.

TABLE A-I

ZrC_x DATA

Analysed	Oxygen (ppm)	Lattice Parameter (nm)	Measured Density Mg m^{-3}	Theoretical Density (Mg m^{-3})	Porosity	Heat Capacity (J kg^{-1} K^{-1})	Measured Thermal Conductivity (W m^{-1} K^{-1})	Thermal Conductivity, Corrected for Porosity (W m^{-1} K^{-1})	Measured Electrical Resistivity (Ωm)	Electrical Resistivity, Corrected for Porosity (Ωm)
1.000[a]	525	0.46988	4.93	6.60	0.25	368	24.5	36.8		
0.982	400	0.46983	6.27	6.60	0.05	368	44.5	48.0		
0.980			5.96	6.60	0.08	368	41.5	44.7		
0.975	260	0.46992	5.38	6.59	0.18	368	28.6	37.3	205	167
0.965	300	0.46992	6.00	6.60	0.09	368	32.2	36.9		
0.946	800	0.46997	5.38	6.56	0.18	367	13.1	17.4		
0.915	870	0.46988	5.60	6.54	0.14	366	12.9	16.1		
0.897	148	0.47014	5.75	6.32	0.12	363	8.9	11.1		
0.870	640	0.47015	5.33	6.50	0.18	362	7.5	9.9		
0.839	380	0.47016	5.54	6.47	0.14	360	7.8	9.7		
0.790	940	0.47013	5.55	6.44	0.14	355	6.2	7.7	296	238
0.750	8100 (1.4675)	0.47149	5.90	6.41	0.08	351	7.3	8.3		
0.743	300	0.47001	6.00	6.41	0.06	351	7.8	8.6	259	237
0.736	200	0.46990	5.12	6.39	0.19	349	5.9	8.0		
0.682	1250	0.46972	6.22	6.37	0.02	343	7.5	7.7	232	222
0.648	420	0.46970	6.17	6.35	0.03	339	8.3	8.7	233	222
0.64	1300	0.46939	6.20	6.35	0.02	339	6.3	6.5		
0.64	1250	0.46955	6.17	6.35	0.03	339	6.5	6.8		

[a] Sample contained 0.5% free carbon.

TABLE A-II

NbC_x DATA

c/Zr Analysed	Oxygen (ppm)	Lattice Parameter (nm)	Measured Density (Mg m^{-3})	Theoretical Density (Mg m^{-3})	Porosity	Heat Capacity (J kg^{-1} K^{-1})	Measured Thermal Conductivity (W m^{-1} K^{-1})	Thermal Conductivity, Corrected for Porosity (W m^{-1} K^{-1})	Measured Electrical Resistivity (Ωm)	Electrical Resistivity, Corrected for Porosity (Ωm)
0.975		0.44700	6.50	7.78	0.16	352	18.8	24.2	114	87
0.925	1600	0.44671	6.49	7.75	0.16	351	11.0	14.1		
0.815	520	0.44519	6.64	7.72	0.14	348	7.7	9.6		
0.702	840	0.44335	6.74	7.72	0.13	329	5.8	7.0		

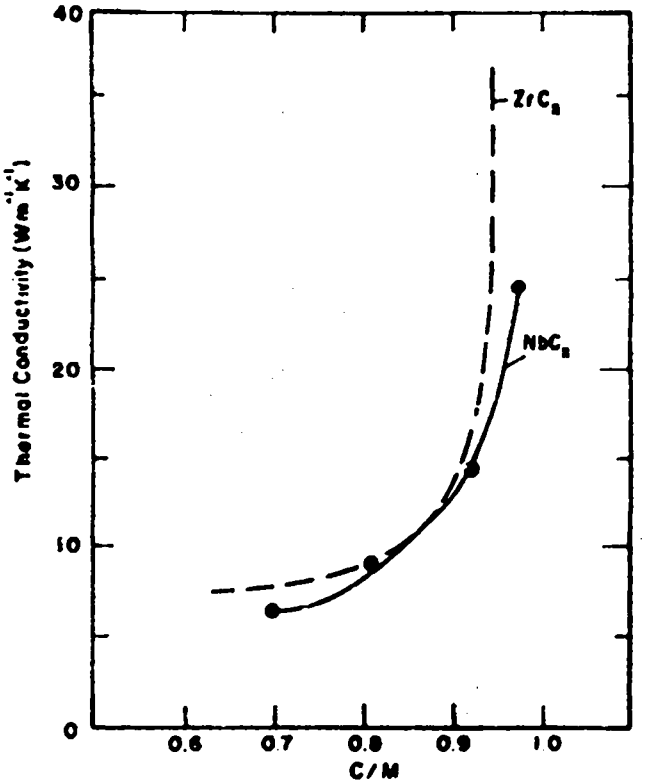

Fig. A-3.
Thermal conductivities of NbC_x (300 K) and ZrC_x (300 K).

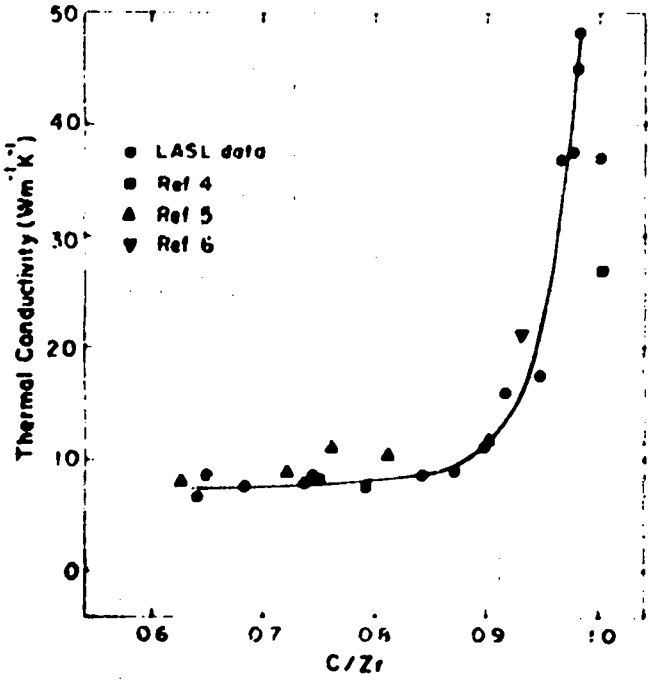

Fig. A-5.
Comparison of LASL thermal-conductivity measurements for ZrC_x at 300 K with literature data.

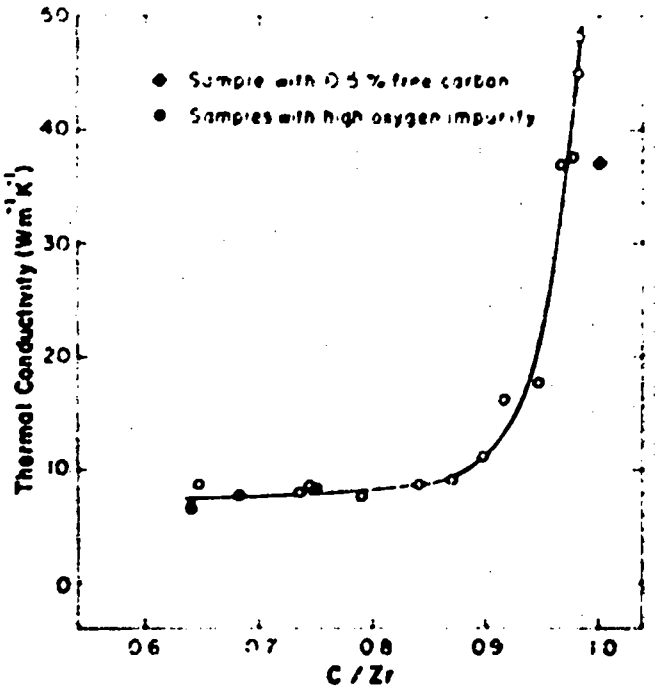

Fig. A-4.
LASL thermal-conductivity data at 300 K for ZrC_x.

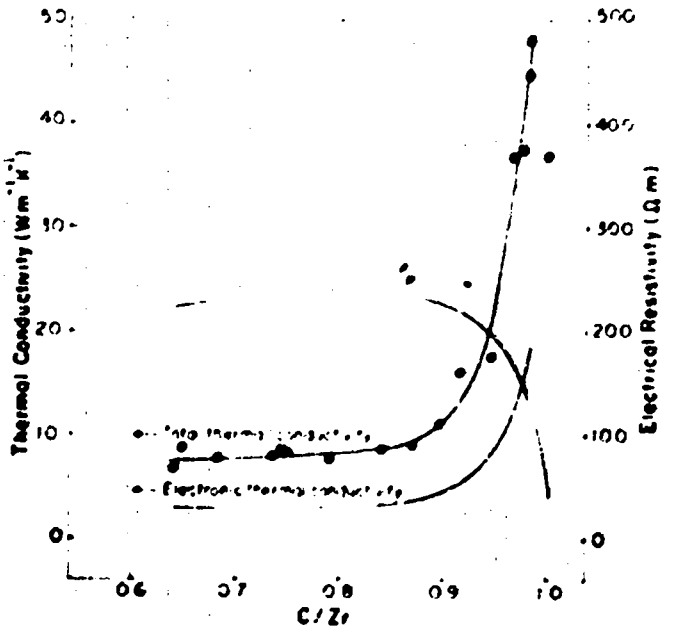

Fig. A-6.
Comparison of total thermal conductivity at 300 K for ZrC_x with electronic component.

REFERENCES

1. P. Wagner and L. B. Dauelsberg, "Thermal Conductivity of ZTA Graphite," Carbon 5, 271 (1967).

2. J. C. Maxwell, *Treatise on Electricity and Magnetism*, (Oxford University Press, London, 1904), Vol. I, 3rd Ed.

3. E. F. Westrum, Jr., and G. Feick, "Zirconium Carbide: Heat Capacity and Thermodynamic Properties from 5 to 350°K," J. Chem. Eng. Data 8, 176 (1963).

4. R. E. Taylor, "Thermal Conductivity of Zirconium Carbide at High Temperatures," J. Amer. Cer. Soc 45, 353 (1962).

5. V. S. Neshpor, S. S. OrJan'yan, A. I. Avgustinik, and M. B. Khusidman, "The Effect of the Chemical Composition of Zirconium and Niobium Carbides in the Homogeneity Region on Their Electric and Thermal Properties," Zhurnal Prikład. Khimii 37, 2375 (1964) (NASA TT F-9350).

6. B. H. Morrison and L. L. Sturgess, "The Thermal Diffusivity and Conductivity of Zirconium Carbide from 100 to 2500 K," Rev. Int. Hautes Temper. et Refract. 7, 351 (1970).

APPENDIX B

FINAL BRIEF SUMMARY OF ZrC INSULATORS FOR THE ROVER PROGRAM

by

J. M. Dickinson, D. H. Schell, and K. V. Davidson

This brief summary of the work on ZrC-related insulator materials in LASL Group CMB-6 is in two sections. The first section discusses material made by hot pressing and the second section discusses extruded insulators.

A. Hot-Pressed ZrC Insulators

The hot-pressing approach was started in 1969 and was continued intermittently until the recent demise of the Rover program. The insulators produced for the program fall generally into two classes—the carbide-oxide mixtures and the porous carbides.

Mixtures of ZrC-ZrO_2 and of HfC-HfO_2 were made at 85% of theoretical density, and thermal conductivities below 2 W/m·K were achieved. The ZrC-ZrO_2 mixture was stable for 8 h at 2575 K and the HfC-HfO_2 was stable for several hours at 2825 K and for 1 h at 3075 K. Details of the procedures and results are reported by Riley and Taub.[1]

Porous hot-pressed ZrC insulators were also investigated during this period with interesting results. By limiting the density to about 40% theoretical, hot pressings having thermal conductivities of less than 2 W/m·K can be made; some have reached less than 1 W/m·K. Control of particle size is particularly important in the porous carbides to obtain low conductivities and some reasonable strength level. These materials appear to be stable for at least 10 h at 2575 K.

Very recently, some studies of $ZrC + ZrO_2 + C$ to give porous ZrC have shown that thermal conductivities of less than 1 W/m·K can be obtained and that thermal conductivities below 2 W/m·K are not uncommon at densities of 50%. These are moderately strong materials and were being considered for hot-end washer applications. The procedures and results of the hot-pressed porous carbides will be described in a later report.

B. Extruded ZrC Insulators

Porous ZrC insulators were made for the Rover program by the extrusion process in an attempt to provide a method for mass producing insulators that would be easier and more reproducible than the hot-pressing method.

We feel that a good insulator should have a microstructure consisting of large, dense ZrC particles with large, clean voids between the particles. Such a structure has been shown to have low conductivity, reasonable strength, and to be thermally stable. The insulators should have thermal conductivities less than 2 W/mK.

Insulators were extruded either as tubes, up to 1.3-cm o.d. or with a rectangular cross section, usually 1 cm by 2 cm.

The following three types of extrusions were made in attempts to obtain the desired microstructure.

1. ZrC at about 60% of theoretical density contained little or no free carbon when heat treated. These extrusion mixes contained ZrC, ZrO_2, carbon, pore former, and binder.

2. Composite extrusions containing 40 to 50% ZrC and from 9 to 24% free carbon when heat treated. The extrusion mixes contained ZrC, carbon, pore former, and binder.

3. Extrusions containing ZrC at 25 to 45% of theoretical density and very little free carbon. These mixes contained ZrC, ZrO_2 carbon, pore former, and binder; or ZrO_2 carbon, pore former, and binder.

A large variety of materials and particle sizes of materials were used to make the insulators. Practically all mixes contained coarse, dense ZrC particles. These

particles were usually in the − 65 to + 150 mesh range, but in some instances were in the − 150 to + 270 mesh range. Particles having such a small range of sizes tend to pack poorly thus leaving large voids between the particles.

The ZrO_2 powder available for most of the development period consisted of fine particles, 1- to 2-μm, or coarser particles that consisted of porous agglomerates of the fine particles. When these particles converted to the carbide they tended to retain their size, shape, and position in the extrusion. The fine ZrO_2 powder ended in voids between the large ZrC particles. The net result was a porous ZrC network in these voids that increased the conductivity of the insulator. This was not always the case because some good insulators were made that contained fine ZrO_2 in the extrusion mix.

Coarse, dense ZrO_2 particles became available late in the development program. These particles, when converting to the carbide, migrated into the surrounding carbon forming a shell of ZrC with a void where the ZrO_2 particle had originally been. This was fortunate in that it provided a method of making stoichiometric extrusions containing large, clean voids.

Free carbon was added to the extrusion mix to aid in the extrusion operation and, in the case of the composite extrusions, to produce discrete voids after the carbon was leached. The carbon added as an extrusion aid was always 200 mesh and for many extrusions was a graphite flour having an average particle size of 0.6 μm. Carbon added to the composite extrusions to create voids was usually smaller than 200 mesh and was either equiaxed graphite flour or spherical particles.

All extrusions contained some pore-forming material that would decompose or vaporize during the insulator heat treatment. Powdered Teflon was the preferred pore former and could be added to the extrusion mix in almost any desired quantity. Pores were desirable in the heat-treated insulators to reduce the overall density, to reduce the amount of carbon in the composite extrusions, and to provide access for the hydrogen leaching gas.

All insulators were extruded using Varcum, a partially polymerized furfuryl alcohol, as the extrusion binder. During heat treatment, the Varcum decomposed leaving a carbon residue.

As mentioned previously, three types of extrusions were made, two of which contained ZrO_2 in the extrusion mix. The main purpose of the ZrO_2 addition was to use up free carbon during the heat-treating operation when the oxide converted to ZrC. This allowed heat-treated extrusions to be made that contained little or no free carbon.

The final insulator could not contain any free carbon. Even a small amount of carbon increased the conductivity dramatically. Therefore, all insulators were leached with hydrogen to remove all traces of free carbon. Normal leaching conditions in LASL Group CMB-6 were 8 h at 2575 K in flowing hydrogen. It proved to be quite difficult and time consuming to leach all of the free carbon from the composite extrusions, although once the carbon was removed, these extrusions made good insulators. Later extrusions concentrated on essentially stoichiometric extrusions made with mixes containing appreciable amounts of ZrO_2.

The following heat-treating procedure was used on the insulator extrusions.

1. Cure (polymerization of the thermosetting Varcum binder) to 520 K for 93 h.

2. Vacuum bake to 1110 K for 48 h.

3 Heat treat to 2775 K and hold at this temperature for 2 h.

Leached insulators were evaluated in relation to density, electrical resistivity, thermal conductivity (diffusivity), and metallography. Some thermal stability and strength measurements were made. Unfortunately this work had barely started when the program was terminated.

A large number (well over a hundred) of insulator extrusion batches were made whose products had conductivities in the 4- to 7-W/mK range. However, several extrusions using a variety of mix formulations had conductivities less than 2 W/mK. In general, the goals of the program were met. Data on selected extrusion batches are tabulated in Table B-I.

REFERENCE

1. R. E. Riley and J. M. Taub, "MC-$M'O_2$ Composites: A New Thermal Insulator," Los Alamos Scientific Laboratory report LA-5136 (February 1973).

TABLE B-I

EXTRUDED ZrC INSULATORS[a]

Batch No.	ZrC Size	ZrO_2 Size	Zr-C-ZrO_2 Ratio	Pore Former (g/cm^3)	Free Carbon and Size	% Free Carbon as Heat Treated	Leached Density		Conductivity (W/mK)
							g/cm^3	%	
4575	-65+150	5.4 μm	75-25	0.10 Teflon	-325+Thermax	None	3.9	60	1.1
5042	-65+150	None		0.10 Teflon	8 μm spherical	17	3.2	49	1.7
5045	-150+270	None		0.10 Teflon	-200+325	16	3.4	51	1.5
5075	-65+150	None		0.10 Reflon	-200+325	24	2.6	40	1.2
5201	None	-150+270		0.10 Teflon	-200+325	24	1.7	25	0.4
5266	-150+270	-200	75-25	0.70 Teflon	0.6 μm	1	2.7	40	0.8
5268	-150+270	-200	50-50	0.70 Teflon	0.6 μm	2	2.6	39	0.8
5270	-150+270	-200	50-50	0.40 Teflon	0.6 μm	2	2.9	43	1.2

APPENDIX C

BRIEF SUMMARY OF NF-2 INSULATOR WORK

by

A. R. Driemer

The NF-2 insulators were manufactured by a process developed in 1971 and early 1972 by Filmore F. Criss of LASL. This process consists of converting carbon-felt cylinders, obtained from the Y-12 Plant at Oak Ridge, to ZrC and then coating each fiber with ZrC. The conversion and coating are done by a vapor deposition process utilizing zirconium tetrachloride

The carbon felt manufactured by Y-12 had a density of about 0.18 g/cm^3. The manufacture of this felt material is described in a Union Carbide Corporation document Y-1803 "Carbon-Fiber Thermal Insulation" by Z. L. Ardary and C. D. Reynolds.

Previous development work at LASL indicated that this carbon felt, when completely converted to zirconium carbide, would have a density of ~1.56 g/cm^3 (24% of theoretical). Although the thermal conductivity in air of this material was quite low (0.4 W/m·K), there was concern that the converted-only material would not possess satisfactory strength to withstand reactor environment and the reactor compressive loads. Consequently, again based on previous development work, a ZrC coating was applied to each fiber to enhance its strength. Because the maximum temperature to which the material was exposed during the conversion-coating process was ~1800 K and the reactor operating maximum temperature was to be ~2750 K, it seemed advisable to heat treat the insulators. This heat treatment was conducted in an argon atmosphere at ~2770 K for 2 h.

The carbon-felt pieces received from Y-12 were ~1-3/8-in. o.d. by 0.6-in. i.d. by 8-in. long. These pieces were premachined to 1.175-in. o.d. by 0.750-in. hex across-flats inside dimension by ~7-5/8 in. long. After machining, all insulator pieces were identified sequentially and were packed 12 each in a styrofoam box. Each box was numbered in the 1000 series.

Each piece was inspected by a DXT device to ascertain density variation along the length of the felt piece and also to check variations between pieces. Figure C-1 shows two typical traces of insulator densities. The calibration units shown on the upper right-hand corner of each trace is the equivalent thickness of carbon felt. In fact, Piece No. 1 was cut to various thicknesses and used as a standard.

Development work on previous carbon-felt pieces indicated that satisfactory thermal conductivity and strength values were obtained if the final density of the ZrC insulator was about 28% of theoretical (1.9 g/cm^3).

Approximately 50 h are required to convert the carbon felt to zirconium carbide. Another 10 h are required for the fiber-coating process.

Following the conversion-coating run, each insulator was heat treated at ~2770 K for 2 h in an argon

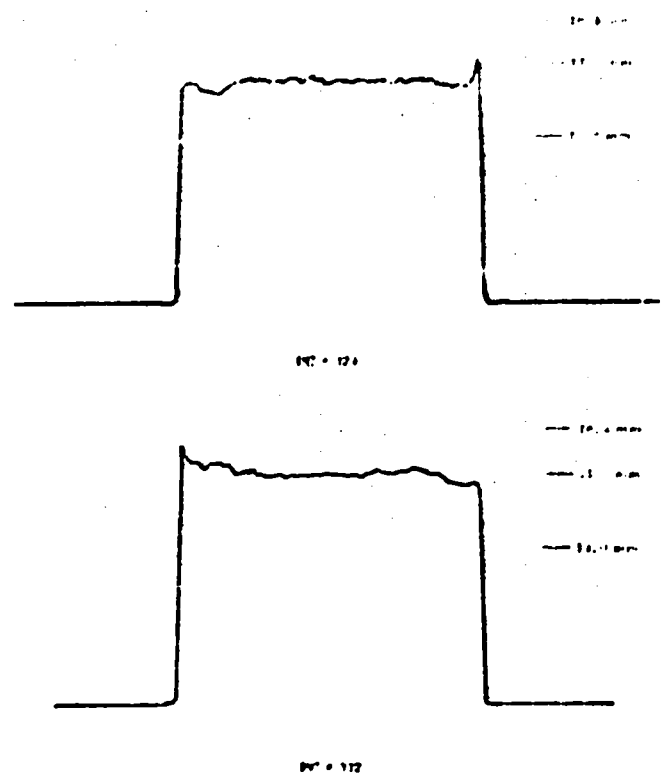

Fig. C-1.
Typical densities of Y-12 carbon felt.

atmosphere. This heat treatment was considered necessary to remove any impurities and to make the insulators dimensionally stable.

Again, each insulator was inspected, nondestructively, for density vs length in a device called MULE (mass per unit length examination). An equivalent density (equivalent to zirconium metal thickness in millimeters) was recorded for each 10 mm of axial length. The first reading is 1 cm from the serial number end of the insulator. The densities for two typical insulators following the conversion-coating run and the heat treatment are shown in Table C-I.

In addition to the density measurements, each insulator was weighed before and after the conversion-coating run and after the heat-treatment run. The data for Runs B3-444 and B2-122 are shown in Table C-II for two typical insulators.

Following the nondestructive testing, the insulators were to be machined to meet NF-2 reactor requirements. Unfortunately, the conversion and heat treating of the insulators had barely been finished when funding for the Rover Program was terminated. Machining requirements for the NF-2 insulators were specified on LASL Drawings 43Y-151129 C2 and C3 but machining was not finished.

A summary of the 11 production batches showing coating and heat-treatment batch numbers plus some technical data are shown in Table C-III.

The density data for Insulator No. 324 shown on Table C-I indicates that the average density was equivalent to 3.104 mm of zirconium metal (density equal to 6.44 g/cm^3). Since the insulator material is ZrC (density equal to 6.61 g/cm^3), if one assumes that the ratio of densities would convert directly to insulator thickness, then the thickness of ZrC would be 3.024 mm. This thickness of ZrC would indicate a theoretical density of 38% since the entire insulator thickness is equivalent to 10.80 mm.

The percent of theoretical density for Insulator No. 324 is 30.8% in Table C-II. However, this number is based

TABLE C-I

EQUIVALENT Zr METAL THICKNESSES OF CONVERTED ZrC INSULATORS

Insulator No. 324 (mm)	Insulator No. 332 (mm)
2.870	2.802
2.835	2.774
2.955	2.733
2.915	2.774
3.010	2.781
3.000	2.813
3.065	2.822
3.086	2.869
3.129	2.899
3.141	2.934
3.191	2.986
3.184	2.949
3.219	2.982
3.184	2.956
3.274	2.984
3.346	3.011
3.356	2.941
Av 3.104	Av 2.883

TABLE C-II

TYPICAL PRODUCTION DATA FOR THE CONVERSION-COATING HEAT-TREAT RUNS

NF-2 Insulators — Boxes 1012 A, B, C, 1013A
Coat Date: 11-27-72 — Bertha Run No. B3-444
Heat-Treat Date: 12-5-72 — Bertha Run No. B2-122

Insulator No.	Box No.	Received Wt, g	Converted Wt, g	Conversion Factors	Percent of T. D.[a]	Heat Treat Wt, g	Heat Treat Loss, g
324	1012A	12.74	140.40	11.02	30.8	139.46	0.94
332	1012B	12.36	124.16	10.05	28.1	12355	0.61

[a]Theoretical Density (calculated from piece volume and weight).

TABLE C-III

NF-2 INSULATOR SUMMARY

Box Number	Quantity	Conversion Batch	Heat Treat Batch	T. D.[a] Percent Av	T. D.[a] Percent Range	Evaluation Pieces	Good Pieces
1003ABC	36	B3-437	B2-112	34.8	32.4 36.4	14	22
1004ABC	36	B4-598	B2-111	27.5	26.4 29.3	12	24
1005ABC 1006A	48	B4-596	B2-113	30.0	27.2 33.1	5	43
1006BC 1007AB	48	B3-440	B2-115	30.8	28.9 34.1	4	44
1007C 1008ABC	48	B3-441	B2-117	28.9	27.2 31.6	1	47
1009ABC 1010A	48	B3-442	B2-119	29.0	25.1 32.6	3	45
1010BC 1011BC	48	B3-443	B2-120	27.3	21.4 31.1	1	47
1012ABC 1013A	48	B3-444	B2-122	27.7	24.4 32.0	1	47
1013BC 1014AB	48	B3-445	B2-124	27.8	22.5 33.4	1	47
1014C 1015ABC	48	B3-446	B2-126	23.6	19.7 24.9	3	45
1016A	12	B3-451	B2-129	30.5	28.1		18
B	6				33.5		
1017A[b]	12			28.2	26.5		24
B[b]	12				29.7		
1018[c]							
	498					45	453

[a] T. D. = theoretical density (calculated from piece volume and weight).

[b] These 24 pieces to be used for 4.4-mm carbide elements.

[c] This box has about 50 unmachined carbon felt pieces.

on nominal dimensions and consequently can be in error, but it was a convenient number to use during insulator production. Had the program continued, each insulator would have been machined to rather closely controlled dimensional tolerances, been weighed, and a revised percent of theoretical density would have been calculated.

Evaluation Data

Approximately 45 insulators were removed from the production pipeline for evaluation purposes, and although all the data and results produced cannot be reported here, a few of the pertinent measurements will be summarized.

Samples

One insulator was taken from each representative production conversion-coating batch and cut into evaluation samples after the heat treatment. These samples included pieces for chemistry, metallography, compressive strength and deformation, and room-temperature thermal conductivity. Unfortunately, the Rover Program termination did not permit completion of the chemistry and metallography samples. However, the strength and thermal-conductivity values were measured on the samples listed in Table C-IV.

CTE

The longitudinal coefficient of thermal expansion was measured on two NF-2 production insulators. One was Piece No. 10 from Box 1003A, which had a density of 2.36 g/cm^3 (35.8% of theoretical density), and the other was Piece No. 55 from Box 1004B, which had a density of 1.76 g/cm^3 (26.7% of theoretical density).

The average coefficient of thermal expansion as measured to 2300 K was

Piece 10:	7.72 μm/m·K
Piece 55:	7.47 μm/m·K

Time did not permit similar measurements in the transverse direction, nor on more pieces, but measurements made in both directions on development material indicated that the material was essentially isotropic.

TABLE C-IV

THERMAL CONDUCTIVITY AND INSULATOR STRENGTH AS A FUNCTION OF THEORETICAL DENSITY

Box Number	Piece Number	Batch Number	Percent of T.D.[a]	Compressive Deformation[b] (% Δl)	Compressive Strength,[c] (psi)	Thermal Conductivity[d] (W/m°K)
1003 B	15	B3-437	36.4	2.3	6526	0.79
1004 A	51	B4-598	27.4	8.5	2450	0.37
1005 A	84	B4-596	31.9	5.2	4317	0.90
1006 B	124	B3-440	34.0			0.87
1007 C	180	B3-441	30.9	10.0	3414	0.72
1009 A	225	B3-442	30.1			1.44
1010 C	282	B3-443	25.0			1.85
1012 B	340	B3-444	26.6	34.	4568	1.99
1013 C	379	B3-445	22.5			1.63
1015 B	442	B3-446	19.7	45.	2108	1.37

[a]T. D. = theoretical density.

[b]Compressive deformation at 2775 K for 1 h at 100 psi load.

[c]Compressive strength of full cross-section sample.

[d]Thermal conductivity as measured in air at room temperature.

Chemistry and Metallography

Chemical analyses were completed on three insulators that had also been used for compressive deformation and strength measurements (Table C-IV).

These insulators had been heat treated and then machined to remove any surface layer effects. The chemical analyses are shown in Table C-V.

TABLE C-V

CHEMICAL ANALYSES OF PRODUCTION INSULATORS

Insulator No.	Ar wt%	C_T wt%	C_F ppm	C to Zr Ratio
1004A-51	89.1	10.58	490	0.90
1005A-84	88.6	11.18	630	0.96
1007C-180	88.8	11.04	410	0.94

Chemistry results indicate that the insulators were slightly substoichiometric and this in turn contributes to the low thermal-conductivity values reported.

Metallographs of these insulators indicate that the entire carbon fiber has been converted to ZrC, very little, if any, free carbon can be seen as substantiated by the chemical analyses. The metallographs also show that the coating process has been applied uniformly across the entire insulator cross section. Each converted fiber had received essentially the same amount of coating. The careful control during the coating process had not resulted in the coating being deposited on the insulator surface to form a "can" coat, but the coating had penetrated completely.

APPENDIX D

CONTRIBUTIONS FOR FINAL INSULATOR REPORT

Design Considerations for Insulator Development

by

T. J. Merson

Introduction

As originally conceived, the program was to provide insulators for three separate applications.

1. Flight reactor tie tube
2. Flight reactor periphery
3. NF-2 cell tubes

Each application had specific design requirements and functions. A later charter was given to consider an insulator for the NF-2 hot-end washer.

Flight Reactor Tie Tubes

The purposes of the tie tube insulators are to

1. Protect the tie tube from excessive temperatures,
2. Reduce heat flux from the fuel (reducing fuel thermal stress),
3. Meter the heat flow to the support system coolant such that the gas exit conditions were proper for turbine operation, and
4. Maintain structural integrity during the life of the reactor.

Specific operating conditions are defined in another Los Alamos Scientific Laboratory report.

Flight Reactor Periphery

The purposes of the insulator for the flight reactor periphery are to

1. Protect the metallic wrapper and beryllium slat from excessive temperatures,
2. Reduce the heat flux from the fuel to the slats, and
3. Support any bundling load that was needed external to the core.

Calculations showing operating conditions are given in another Los Alamos Scientific Laboratory report.

NF-2 Cell

The purposes of the insulators in the NF-2 cells are to

1. Reduce heat loss from the fuel
   a. To reduce fuel thermal stresses
   b. To keep the aluminum cell tube temperatures below redline with the limited water cooling rates available, and
2. Provide some radial mechanical support to the fuel element.

Design calculations are presented in several LASL internal documents for effect of thermal conductivity, 19-hole carbide cluster, thermal stress, axial expansions, size calculations, and effect of thermal transients.

NF-2 Hot-End Washer

The purpose of the hot-end washer is to provide a temperature transition and thermal impedance from the hot fuel and support tip to the aluminum tube bundle. This insulator had a compressive strength requirement because it took the entire fuel pressure drop while at operating temperature.

U.S. Government Printing Office: 1992-673-036/67031